Mineralogical Magazine (2019), **83**, 161–179
doi:10.1180/mgm.2018.151

CAMBRIDGE UNIVERSITY PRESS

Article

The geochemical evolution of Nb–Ta–Sn oxides from pegmatites of the Cape Cross–Uis pegmatite belt, Namibia

Warrick C. Fuchsloch*, Paul A. M. Nex and Judith A. Kinnaird
School of Geosciences, University of the Witwatersrand, South Africa

Abstract

The Cape Cross–Uis pegmatite belt, Damara Orogen, north-central Namibia hosts multiple Ta–Nb- and Sn-oxide-bearing pegmatites. Columbite-group minerals, tapiolite, cassiterite and minor ixiolite and wodginite occur in abundance within pegmatites and display various compositional and internal structural mineralogical variations. Ta–Nb oxides display various zonation patterns indicative of multiple crystallisation phases, whereas cassiterite is dominantly homogeneous with minor euhedral columbite-group mineral inclusions. Ta–Nb oxides are mostly rich in Fe, with fractionation patterns in the columbite quadrilateral being sub parallel to the Ta/(Ta + Nb) axis; increasing Ta/(Ta + Nb) with little change in Mn/(Mn + Fe), which is consistent with classical trends in beryl-to-spodumene rare-element pegmatites. In addition, these trends suggest that co-crystallising minerals compete with Ta–Nb oxides for elements such as Mn, preventing Ta–Nb oxides from attaining Mn-rich compositions during the fractionation process. Cassiterite shows similar fractionation patterns with Fe > Mn and notable increases in the Ta content. Minor-element substitution in Ta–Nb oxides shows sharp decreases with increasing fractionation supporting the hypothesis that newly stabilised co-occurring minerals compete with columbite-group minerals for certain elements. Tapiolite shows the same minor-element trend, however, only for Sn and Ti suggesting cassiterite was a dominant competing mineral. Although crystallisation of Ta–Nb oxides from an aqueous fluid at the late-stages of pegmatite genesis is highly debated, significantly elevated Ta contents in metasomatised country rock, compared to unaltered country rock, may give new insight, suggesting that Ta may indeed partition into, and be transported by, an exsolved aqueous fluid. However, further studies of the country rock metasomatic contacts are required as currently the dataset is limited. The degree of fractionation as depicted by Ta–Nb and Sn oxides within pegmatites, indicate that a zonation from primitive to evolved pegmatites surrounding granites is not present and that pegmatites are probably not related to granites in the typical parent–daughter relationship.

Keywords: columbite-group minerals, tapiolite, cassiterite, granitic pegmatite, Damara Orogen, Namibia

(Received 16 February 2018; revised 30 July 2018; accepted 6 August 2018)

Introduction

The internal evolution processes of a pegmatite-forming magma, such as fractionation (Černý and Ercit, 1985; Mulja *et al*, 1996; Novák and Černý, 1998; Martins *et al*., 2009) and crystallisation conditions (Ercit *et al*., 1995; Van Lichtervelde *et al*., 2007) can be traced using the composition of Ta–Nb–Sn oxides. While many studies have focused on the pegmatite or crystal scale (Lahti, 1987; Splide and Shearer, 1992; Hanson *et al*., 1998), new data have begun to emerge in which compositional databases for columbite-group minerals [$(Fe,Mn)(Ta,Nb)_2O_6$] are based on a group, or a district and may even cover the continental scale (Alfonso *et al*., 1995; Tindle and Breaks, 2000; Beurlen, 2008; Melcher *et al*., 2013, 2015, 2017). In addition, columbite-group minerals have been the subject of many experimental studies (e.g. Černý *et al*., 1992*b*; Linnen *et al*., 1996; Linnen and Keppler, 1997; Linnen, 1998), have been used in conjunction with whole-rock pegmatite geochemistry (Raimbault, 1998) and have even been used for radiometric age determination (Romer and Lehmann, 1995; Smith *et al*., 2004; Baumgartner *et al*., 2006; Van Lichtervelde *et al*., 2017).

In the Cape Cross–Uis pegmatite belt of Namibia, numerous granitic pegmatite bodies intrude the metasedimentary and granitic rocks of the Zerrissene Group and Salem-type granites. These pegmatites have been mined sporadically for Li, Sn, Ta and Nb. Fuchsloch *et al.* (2018) have reported in detail on the field characteristics, mineralogy and whole-rock geochemistry of pegmatites from the Cape Cross–Uis pegmatite belt. These pegmatites show a wide variety of characteristics in terms of intrusion dimensions, complexity, mineralogy, mineralisation and whole-rock geochemistry, throughout the 120 km long by 40 km wide area (Richards, 1986; Diehl, 1993; Fuchsloch *et al*., 2018).

Regardless of the emergence of district and continent scale columbite-group mineral compositional databases (Wise *et al*., 2012; Melcher, *et al*., 2013, 2015), many pegmatite groups have not yet been studied in detail. The objective of this paper is to present the first detailed compositional study of columbite-group minerals, tapiolite and cassiterite from the Cape Cross–Uis pegmatite belt. High definition back-scattered electron (BSE) images combined with mineral geochemical data are used to evaluate the fractionation trends within the pegmatites at all scales from an individual crystal through the pegmatite body, to a regional pegmatite-belt scale. An evaluation of the degree of fractionation

***Author for correspondence:** Warrick C. Fuchsloch, Email: wfuchsloch@gmail.com
Associate Editor: Sam Broom-Fendley
Cite this article: Fuchsloch W.C., Nex P.A.M., Kinnaird J.A. (2019) The geochemical evolution of Nb–Ta–Sn oxides from pegmatites of the Cape Cross–Uis pegmatite belt, Namibia. *Mineralogical Magazine* **83**, 161–179. https://doi.org/10.1180/mgm.2018.151

gives insight into the granite–pegmatite relationship, which Fuchsloch *et al.* (2018) found questionable, suggesting an anatexis model for pegmatite petrogenesis rather than fractionation from a parent granite body. Crystallisation conditions and paragenetic sequences of crystallisation of columbite-group minerals and cassiterite are also assessed by evaluating the heterovalent substitutions in these minerals.

Geological setting

Regional overview

Several rare-element pegmatite belts in Namibia occur within the Damara Belt, which is the northeast-trending intracontinental branch of the Neoproterozoic Pan-African Damara Orogen (See Richards, 1986 and Keller *et al.*, 1999; Fig. 1). The Damara Belt extends from the Atlantic coast near Swakopmund inland towards Botswana and represents a typical 'Wilson Cycle' between 750 Ma to 440 Ma, which culminated in the collision of the Kalahari and Congo cratons (Martin and Porada, 1977; Hoffman *et al.*, 1996; Prave, 1996; De Kock *et al.*, 2000; Gray *et al*, 2006; Miller, 2009). On the basis of structure, stratigraphy, igneous activity and metamorphic grade, Miller (1983, 2008 and 2009) divided the Damara Belt into a number of tectonostratigraphic zones bound by major lineaments and faults (Fig. 1). The Cape Cross–Uis pegmatite belt is located in the Northern Zone of the Damara Belt, which is bound by the Autseib fault and the Otjihorongo thrust (Figs 1, 2).

During the stages of extension, spreading, subduction and final continental closure, various sedimentary, volcanic and intrusive rocks were formed that represent the magmatism in the polydeformed and polymetamorphic Damara Belt (Prave, 1996; Trompette, 1997). Initial Damaran intrusive magmatism was triggered by subduction which occurred between 580 Ma and 545 Ma and is represented by the Goas Suite (Milani *et al.*, 2015). The final deformation event, D_3, has been determined radiometrically to be between 542 and 519 Ma and is responsible largely for the voluminous granodioritic and granitic magmatism during the orogenesis stages of the Damara Belt (Tack *et al.*, 2002; Kisters, 2005; Longridge, 2012). Pegmatites form part of this magmatic episode and are ubiquitous within the Damara Belt. They were emplaced within the time period 509–429 Ma (Briqueu *et al.*, 1980; Longridge, 2012), however, economic mineralisation appears to be exclusively post-tectonic (Wagener, 1989; Diehl, 1993; Kinnaird and Nex, 2007; Miller, 2008; Longridge, 2012; Ashworth, 2013).

The Cape Cross–Uis pegmatite belt

Pegmatites of the Cape Cross–Uis pegmatite belt intrude metasediments and granites of the Northern Zone, which is dominated by the Amis River Formation of the Zerrissene Group (Fuchsloch *et al.*, 2018). Granites are fine- to coarse-grained, porphyritic granodiorites of the Salem type and monzogranites of the Red and Grey granites. Metasedimentary rocks represent a fan fringe deposit and consist typically of biotite schist ± cordierite porphyroblasts and minor metagreywacke and quartzite units (Swart, 1992). Metasedimentary rocks show both earlier regional metamorphism to greenschist facies and later thermal metamorphism induced by the intrusion of Salem-type granites (Goscombe *et al.*, 2004). Structural features of the area are characterised by moderately- to steeply-inclined, north–south-striking folds (Macey and Harris, 2006). However, Fuchsloch *et al.* (2018) show that pegmatites are exclusively post-tectonic and were emplaced into pre-existing north-northeast structural weaknesses in the crust.

The pegmatite belt is divided into three pegmatite swarms known as the Strathmore, Karlowa and Uis swarms (Fig. 2). Diehl (1993) suggested that increased Sn mineralisation in pegmatites coincides with an increase in the metamorphic grade to the west. Fuchsloch *et al.* (2018) found no evidence for the westward increase of the mineralisation grade but instead describes different features in the swarms. The authors found that the Uis pegmatites show the highest cassiterite abundances whereas the Karlowa pegmatites are Li-Nb-Ta rich with spodumene occurring as the dominant Li mineral. Furthermore, the Strathmore pegmatites show enrichment in Li, Ta, Nb, Sn and Be with petalite occurring as the dominant Li mineral. Strathmore is the only swarm in which complex mineralogically zoned pegmatites occur, for example, the Petalite pegmatite (Fig. 2).

Pegmatites in the Cape Cross–Uis pegmatite belt are classified as LCT type (lithium, caesium and tantalum) based on the classification of Černý and Ercit (2005). Some pegmatites show the hallmarks of LCT-type pegmatites whereas others, such as the intragranitic garnet–tourmaline pegmatites, show intermediate characteristics between NYF (niobium, yttrium and fluorine) and LCT pegmatite types. Shortcomings in the current classification schemes have led authors such as Fuchsloch *et al.* (2018) to subdivide the pegmatites of the Cape Cross–Uis pegmatite belt into three separate groups based on geochemical and mineralogical characteristics: (1) the barren to Nb–Ta–Sn-mineralised, unzoned pegmatites; (2) garnet–tourmaline, intragranitic, crudely zoned pegmatites; and (3) zoned and unzoned Li-mineralised pegmatites. The petrology and characteristics of the pegmatite groups are well documented (Richards, 1986; Wagener, 1989; Diehl, 1993; Ashworth, 2013; Fuchsloch *et al.*, 2018). Table 1 assigns the pegmatites studied to these different groups. The bulk mineralogical composition of the pegmatites is granitic, with quartz, muscovite, albite and microcline as essential minerals. Primary accessory mineralogy varies between the pegmatite groups and includes columbite-group minerals cassiterite, tapiolite, magnetite, ilmenite, tourmaline, apatite, beryl, petalite, lepidolite, spodumene, zircon and monazite. Secondary mineralogy includes cleavelandite, hectorite, eucryptite and alteration zones of muscovite, quartz and albite.

Various authors, such as Richards (1986), suggest that pegmatites of the Damara Belt are associated with I- and S-type granitic and granodioritic intrusions. However, Fuchsloch *et al.* (2018) questioned this relationship and showed, using the spatial distribution of pegmatites of the Cape Cross–Uis pegmatite belt together with whole-rock geochemistry, that a parent–daughter relationship between granites and pegmatite is unlikely. Fuchsloch *et al.* (2018) favours an anatexis model for pegmatite petrogenesis. Rb–Sr radiometric age determination of the Uis pegmatites is 496 ± 30 Ma and 486 ± 8 Ma by Haack and Gohn (1988) and Diehl (1993), respectively. Richards (1986), Wagener (1989), Diehl (1993) and Singh (2007, 2008) agreed that mineralisation of elements such as Sn was controlled by assimilation of country rock. However, Fuchsloch *et al.* (2018) shows, using field evidence and whole-rock geochemistry, that assimilation was not likely to have been the cause of mineralisation and that internal pegmatite fractionation was the dominant process leading to Nb, Ta, Cs and Sn enrichment.

Late-stage greisenised and albitised zones contain Ta–Nb and Sn oxides in abundance although they also occur in magmatic zones with an equigranular magmatic texture (Table 1; Fuchsloch *et al.*, 2018). These alteration zones which have been shown to

https://doi.org/10.1180/mgm.2018.151 Published online by Cambridge University Press

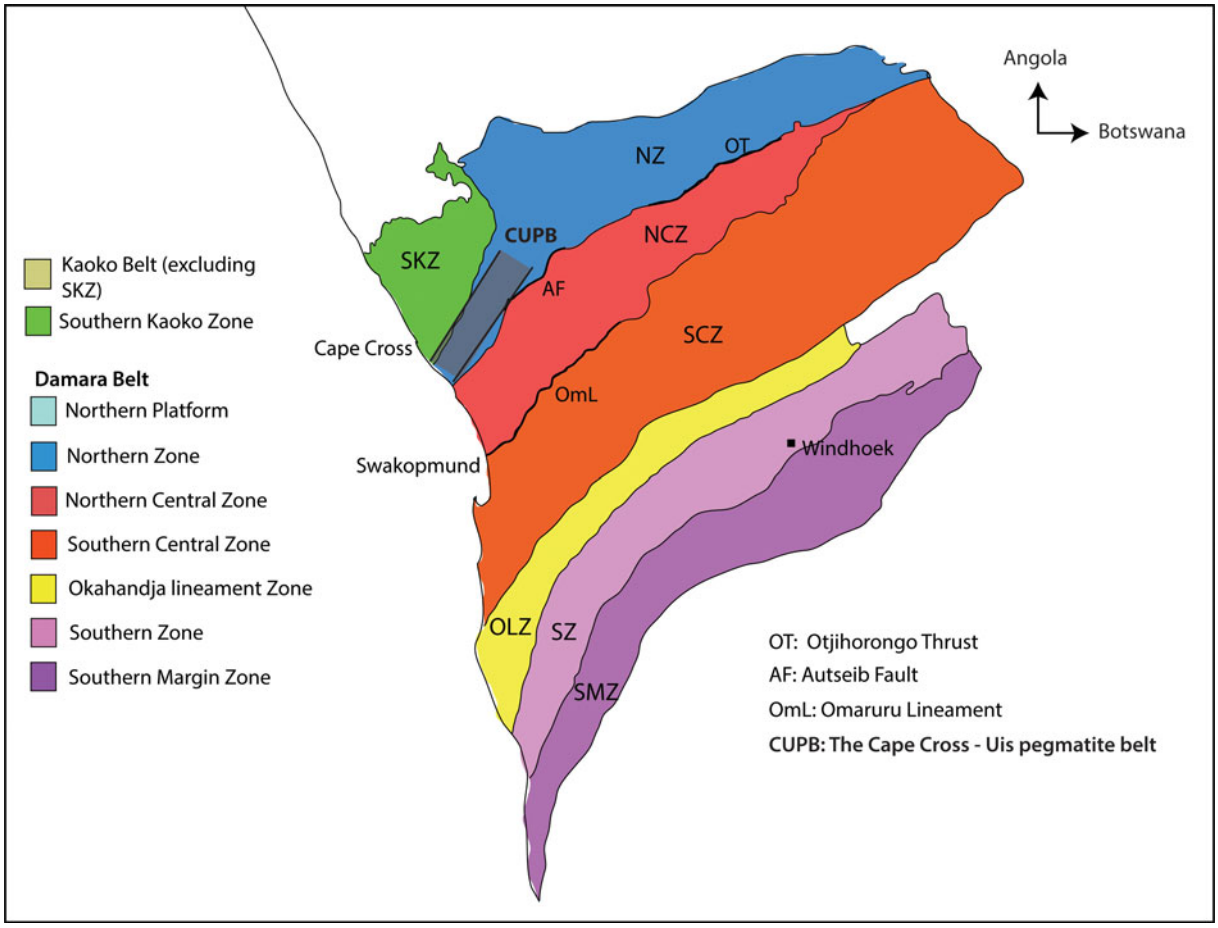

Fig. 1. The Damara Belt showing the different stratigraphic zones defined by Miller (2008) (modified after Miller, 1983 and Fuchsloch *et al.*, 2018).

have the highest levels of fractionation in terms of whole-rock geochemistry, occur sporadically, or in discrete zones, within pegmatites and are not restricted to a pegmatite type. Columbite-group minerals occur in all the different pegmatite types in the Cape Cross–Uis pegmatite belt but to a lesser extent in the garnet–tourmaline pegmatites as only one such pegmatite was found to have columbite-group minerals (Fuchsloch *et al.*, 2018). Cassiterite occurs sporadically in different pegmatites, is completely absent from the garnet–tourmaline type and is abundant in the Uis swarm. Previous studies (Melcher *et al.*, 2013, 2015) and this present investigation have reported the occurrence of other Ta–Nb oxides such as tapiolite, ixiolite and wodginite, on the basis of compositions obtained by microprobe. Melcher *et al.* (2013, 2015) suggests that the Uis pegmatites and the C1 pegmatite (Fig. 2) show concomitant Fe–Mn and Nb–Ta fractionation trends (increasing Ta/(Ta + Nb) and Mn/(Mn + Fe) in a 1 to 1 ratio) in columbite-group minerals, which is typical of the complex spodumene pegmatite type. However, that study is on a continental scale and lacks the detailed investigation of this report.

Sampling and analytical techniques

Twenty-five different pegmatite bodies were sampled in 20 different pegmatite locations in the Cape Cross–Uis pegmatite belt (Fig. 2). Although the pegmatites are predominantly unzoned (Fuchsloch *et al.*, 2018), samples were selected from greisenised zones, albitised zones and magmatic zones with a magmatic equigranular texture. Each sample was crushed, milled and sieved to <500 μm grain size and then processed on a Wilfley table. Samples were further processed using a Franz magnetic separator. These processes extracted the heavy and magnetic mineral populations that were then mounted into resin blocks for electron microprobe analysis. All samples yielded columbite-group minerals ± tapiolite, whereas cassiterite was only recovered in 15 samples (Table 1).

Five hundred and thirty five quantitative compositional analyses for columbite group minerals, tapiolite and cassiterite were obtained using a JEOL JXA-8230 electron micro-analyser with four wavelength dispersive spectrometers at Rhodes University. The electron beam was generated by a tungsten cathode at 30 nA current with a 1 μm beam size. X-ray counts for Mg, Fe, Ca, Mn, Ti and Sc were measured on *Kα* peaks, Sn, W and Nb on *Lα* peaks and U and Ta on *Mα* peaks. Counting times were 10 s on the peak and 10 s total on the background, for all elements. Standards used were: Sn – metallic Sn; Ta – metallic Ta; U – metallic U; Ca/W – scheelite; Mg/Fe – chromite; Mn – rhodonite; Nb – metallic Nb; Ti – rutile; and Sc – metallic Sc. Calibration acquisitions were peaked on the standards whilst unknown acquisitions were peaked on the samples before each point analysis. The data were collected with *JEOL* software. An automated *ZAF* matrix algorithm was applied to correct for differential matrix affects.

Individual, complexly zoned, tapiolite crystals and cassiterite crystals were analysed using a Cameca SX100 electron microprobe at the Natural History Museum, London. Eighty seven points on 15 tapiolite crystals and 24 points on five cassiterite crystals for

https://doi.org/10.1180/mgm.2018.151 Published online by Cambridge University Press

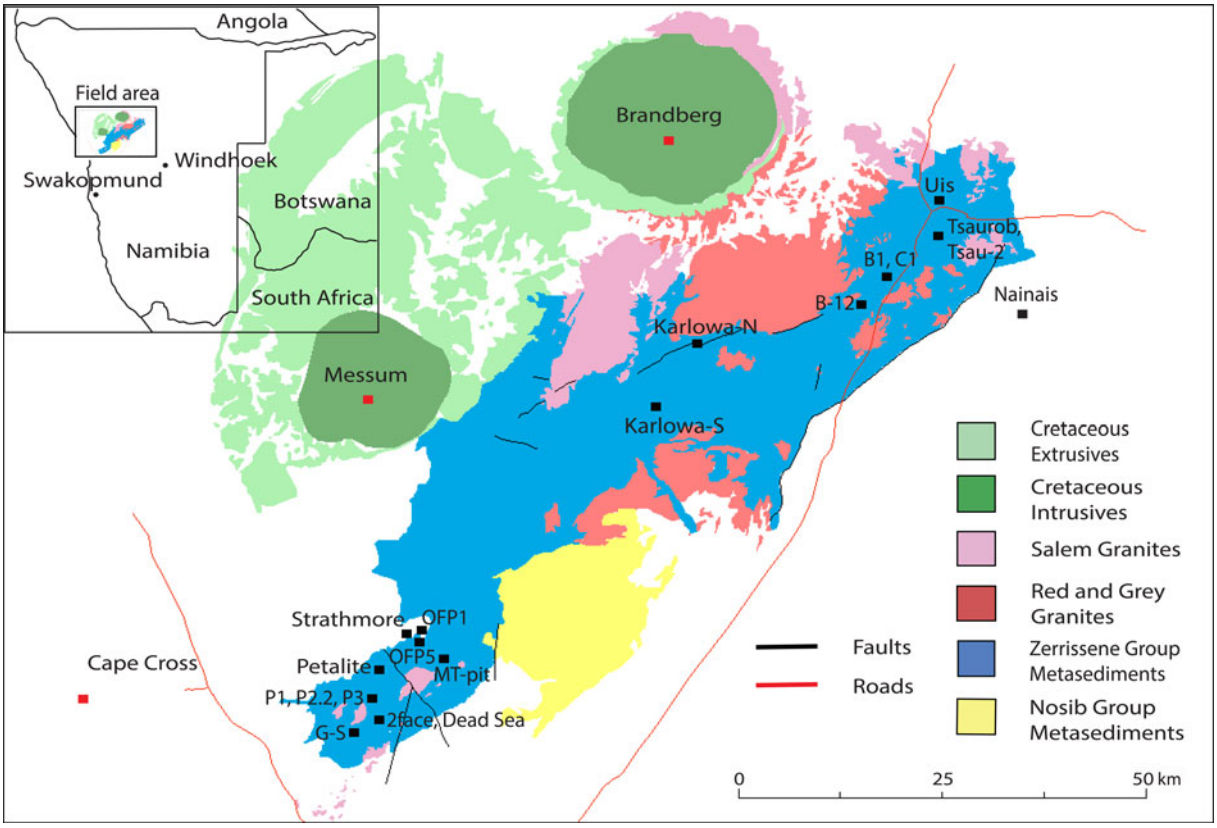

Fig. 2. A simplified geological map of the Cape Cross–Uis pegmatite belt, Namibia (modified after Fuchsloch *et al.*, 2018). The black squares show the approximate locations of the twenty pegmatite areas that were sampled. Twenty five individual samples were collected from these pegmatites. Pegmatites in the southwest are part of the Strathmore swarm, those in the Karlowa area are part of the Karlowa swarm and those in the northeast are part of the Uis swarm.

samples 3.1-2 and 6-1, respectively, (Table 1) were analysed. A current of 20 nA was used with an accelerating potential of 20 keV, a beam size of 1 μm and various counting times ranging from 10–60 s. Counts for Na, Mg, Al, Si, Ca, Ti, Mn, Fe and Sc were measured on *Kα* peaks, Nb, Sn, Zr, Ta, Hf and W on *Lα* peaks and U and Th on *Mα* peaks. Standards used were: Na – jadeite; Mg – forsterite; Al – corundum; Si/Ca – wollastonite; Nb –metallic Nb; Sn – cassiterite; Ti – rutile; Mn – manganese titanium oxide; Fe – haematite; Zr – zircon; Ta –metallic Ta; Hf – metallic Hf; Th – monazite; U – uranium oxide; W – pure tungsten; and Sc – metallic Sc. The data were collected on Cameca software and a *ZAF* matrix algorithm was used to correct for differential matrix affects. Oxygen was calculated using stoichiometry and the atoms per formula unit (apfu) were calculated based on 3 cations and 6 oxygens pfu for all data collected.

The data collected were screened to ensure that only columbite-group minerals, tapiolite and cassiterite were evaluated, as wodginite and ixiolite are very minor constituents or are completely absent from most pegmatites and therefore are beyond the scope of this study. The data were plotted on a Nb *vs*. Ta diagram (Fig. 3) where ideal columbite-group mineral and tapiolite compositions should plot within a boundary between Nb + Ta = 2.0 apfu and Nb + Ta = 1.8 apfu. Ideal compositions refer to the correct stoichiometric proportions of Nb to Ta in a given crystal that constitutes the specific crystal being of the columbite-group minerals (Neiva, 1996). Ten data points plotted below this boundary and are considered to belong to the wodginite and ixiolite family as defined by Neiva (1996). Table 1 shows the Ta–Nb and Sn oxide mineralogy of each pegmatite.

Results

Columbite-group minerals and cassiterite are the dominant Ta–Nb–Sn-bearing phases in the Cape Cross–Uis pegmatite belt. Subordinate tapiolite, wodginite and ixiolite occur but have not been observed macroscopically and have restricted distributions occurring only in highly altered zones of the pegmatites. Wodginite and ixiolite were only identified from their composition as analysed by microprobe, whereas tapiolite has been observed microscopically, only as a secondary phase in all samples except in sample 3.1-2 (Table 1). Although many samples include Ta–Nb–Sn-bearing phases in magmatic zones with a distinct equigranular texture, they are more abundant in greisenised or albitised zones within the pegmatites. These altered zones do not indicate that the pegmatite itself is zoned; only the Petalite pegmatite shows a true mineralogical zonation (Fig. 2; Table 1). The greisens consist essentially of new or recrystallised quartz and muscovite, with accessory columbite-group minerals, tapiolite and cassiterite. They were formed by late-stage pegmatitic fluids and show varying degrees of alteration. They occur as patchy networks, layered units, or in the case of the Petalite pegmatite, as large metre-scale zones surrounding the quartz core of the pegmatite. Their sizes range from several centimetre patches, occurring sporadically in pegmatites, to metre-scale lensoidal or layered units. Albitised zones share similar features to greisens but consist of a homogeneous mass of saccharoidal albite. Ta–Nb–Sn-bearing phases show varying grain sizes in greisens but are mostly macroscopic whereas albitised zones rarely display distinguishable grains.

https://doi.org/10.1180/mgm.2018.151 Published online by Cambridge University Press

Table 1. Ta–Nb and Sn oxides and characteristics of pegmatites studied in the Cape Cross–Uis pegmatite belt (shown in Fig. 1).

Pegmatite	Sample #	Pegmatite type	Ta–Nb–Sn oxides	Oxide occurrence	Columbite-group mineral zonation
G-S	12-1	Grt–Tur	FeC, MnC, Cst	Magmatic zone	Oscillatory
Dead Sea	2-4	Nb–Ta–Sn	FeC	Magmatic zone	Progressive
Nainais	Na-5	Nb–Ta–Sn	FeC, FeT, Cst	Magmatic zone	Oscillatory, patchy
	Na-6	Nb–Ta–Sn	FeC, FeT, Cst	Magmatic zone	Progressive
Petalite	G-4	Li pegmatite	FeC, Cst	Greisen zone	progressive
Strathmore	4-3	Nb–Ta–Sn	FeC, FeT	Magmatic zone	Progressive
	4-4	Nb–Ta–Sn	FeC	Albitised zone	Progressive
	4-9	Nb–Ta–Sn	FeC, FeT, MnC	Magmatic zone	Oscillatory
	4-11	Nb–Ta–Sn	FeC, MnC, Tap	Magmatic zone	Oscillatory
	4-12	Nb–Ta–Sn	FeC	Magmatic zone	Progressive
2face	10-4	Nb–Ta–Sn	FeC, FeT	Magmatic zone	Progressive
Tsau-2	J-5	Nb–Ta–Sn	FeC, FeT, MnC, Cst	Magmatic zone	Oscillatory, patchy
OFP5	B-2	Nb–Ta–Sn	FeC, FeT, MnC, Cst, Wdg/Ix	Greisen zone	Oscillatory, patchy
C1	W-3	Nb–Ta–Sn	MnC, MnT, Tap	Greisen zone	Oscillatory, patchy
OFP1	A-2	Nb–Ta–Sn	FeC, FeT, Cst	Magmatic zone	Oscillatory
B1	X-1	Nb–Ta–Sn	FeC, FeT, MnC, MnT, Tap, Cst	Greisen zone	Complexly zoned
B-12	M-2	Nb–Ta–Sn	FeT, FeC, Tap, Wdg/Ix, Cst	Greisen zone	Complexly zoned
Tsaurob	T-4	Nb–Ta–Sn	FeC, FeT, Cst	Magmatic zone	Oscillatory
P2.2	3-3	Nb–Ta–Sn	FeC, FeT, Cst	Magmatic zone	Progressive
P3	3.2-1	Nb–Ta–Sn	FeC, Cst	Magmatic zone	Progressive
Karlowa-S	5-3	Li pegmatite	FeC, FeT, Tap, Cst	Magmatic zone	Oscillatory, patchy
Karlowa-N	5.1-1	Li pegmatite	Tap, Cst	Greisen zone	Progressive
Uis	6-1	Nb–Ta–Sn	Cst, (CGM inclusions)	Magmatic zone	Oscillatory
MT-pit	D-4	Nb–Ta–Sn	FeC, FeT	Magmatic zone	Oscillatory
P1	3.1-2	Nb–Ta–Sn	Tap	Greisen zone	Complexly zoned

Grt–Tur = garnet–tourmaline pegmatite type; Ta–Nb–Sn indicates the unzoned Ta–Nb–Sn mineralised pegmatites; Li pegmatites indicate the unzoned and zoned Li-mineralised pegmatites. FeC = columbite-(Fe); FeT = tantalite-(Fe); MnC = columbite-(Mn); MnT = tantalite-(Mn); Cst = cassiterite; Tap = tapiolite; Wdg = wodginite; Ix = ixiolite; CGM = columbite-group minerals.

Most Ta–Nb and Sn oxide studies (e.g. Černý *et al.*, 2004) are related to complexly zoned pegmatites, each zone having uniquely occurring Ta–Nb–Sn-bearing phases with distinct compositions. Although only one pegmatite shows true pegmatite zonation in this study, in other examples, a comparison between magmatic and altered zones yields a similar distinction in characteristics and mineralogy of Ta–Nb–Sn oxides. The whole-rock geochemical and mineralogical differences in these zones have already been characterised by Fuchsloch *et al.* (2018).

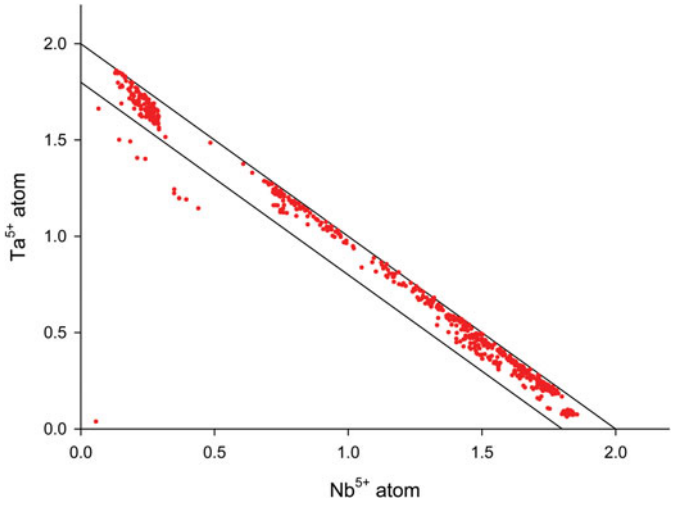

Fig. 3. The atomic proportions of Ta and Nb of the columbite-group minerals and tapiolite from the Cape Cross–Uis pegmatite belt. Points that plot below the boundary are considered to be of the wodginite and ixiolite family. Points within the boundary are considered to be of ideal columbite-group mineral compositions where Ta and Nb are in the correct proportions to constitute the columbite-group mineral (Neiva, 1996; Tindle and Breaks, 2000).

Columbite-group minerals have the general formula of AB_2O_6 where the *A* site is occupied mostly by Fe and Mn and the *B* site mostly by Ta and Nb. The columbite-group minerals comprise four end-members all with an orthorhombic crystal structure: columbite-(Fe) [$FeNb_2O_6$], tantalite-(Fe) [$(Fe > Mn)(Ta > Nb)_2O_6$], columbite-(Mn) [$MnNb_2O_6$] and tantalite-(Mn) [$MnTa_2O_6$]. Tantalite-(Fe) only requires Fe > Mn and Ta > Nb as the composition $FeTa_2O_6$ belongs to the tetragonal tapiolite series and does not exist in the orthorhombic crystal structure of columbite-group minerals (Černý *et al.*, 1992*b*). The overall proportions of Ta to Nb and Fe to Mn [Ta/(Ta + Nb), Ta#; Mn/(Mn + Fe), Mn#] in the columbite quadrilateral are used to show fractionation trends within pegmatite bodies where various different trends may be observed and linked to certain petrochemical processes and abundances (e.g. Černý and Ercit, 1985; Tindle and Breaks, 2000). An increase in Ta# in columbite-group minerals, and in tapiolite and cassiterite is widely accepted as an indication of higher levels of fractionation whereas changes in the Mn# are debated (see discussion in Van Lichtervelde *et al.*, 2007). Columbite-group minerals, tapiolite and cassiterite compositional data were used to evaluate fractionation trends within pegmatites of the Cape Cross–Uis pegmatite belt. Element substitution by Ti, Ca, W, Mg and Sn was also assessed. The data were then used to compare compositions from different pegmatite groups and swarms in the Cape Cross–Uis pegmatite belt. The shape of certain fractionation trends in the columbite quadrilateral for columbite-group minerals have also been used as a classification tool (Černý and Ercit, 1989).

Columbite-group minerals and tapiolite

Occurrence and internal structure

Columbite-group minerals in the Cape Cross–Uis pegmatite belt occur in various morphologies depending on their location within a given pegmatite and are the most abundant Ta- and Nb-bearing

https://doi.org/10.1180/mgm.2018.151 Published online by Cambridge University Press

phases. The most common occurrence of columbite-group minerals is in the form of platy striated black crystals with a metallic lustre which can either occur as amalgamated laths, several centimetres long or as single plates with smaller grain sizes between 100 and 500 μm. The largest amalgamated crystals occur in the unaltered magmatic zones of the pegmatite whereas the equigranular plates occur mostly in the alteration zones. Large tabular crystals are rare but have also been noted. The columbite-group minerals occur uniformly throughout the Cape Cross–Uis pegmatite belt and no swarm in particular favours higher abundances. The most common end-member in the Cape Cross–Uis pegmatite belt is columbite-(Fe) followed by tantalite-(Fe). Manganese end-members are rare but are present in several samples, particularly in greisens (Table 1). Tapiolite forms exclusively anhedral crystals up to 0.5 mm in size and similarly to manganese end-members are rare, with only one sample having abundant tapiolite (Sample 3.1-2; Table 1).

The internal structure of columbite-group minerals and tapiolite shows multiple, singular and/or complex zonation patterns (Fig. 4). The columbite-group minerals are sometimes associated with cassiterite either enclosing cassiterite grains or co-occurring with cassiterite (Fig. 4*a*). The complexity of zonation in a single crystal corresponds to the degree of alteration in the pegmatite zone in which the crystal occurs. The most complex-zoned crystals occur in the latest-stage zones. Zonation patterns in columbite-group minerals and tapiolite have been compared to typical feldspar zoning of which there are three dominant types (Lahti, 1987).

The most common type of zonation seen in the Cape Cross–Uis pegmatite belt is a progressive zonation whereby crystals, from core to rim, have a mono-directional compositional variation that can either be in a single direction (Fig. 4*b*) or concentrically arranged (Fig. 4*c*). Each subsequent zone that crystallised can show either a progressive increase in Ta or Nb, from core to rim. Subsequently crystallised zones may not show alternating increases and decreases of Ta or Nb, which would be considered oscillatory zonation. Within each individual zone (e.g. Fig. 4*b* has four individual zones), slight changes in the BSE images brightness show that progressive zonation may occur within individual zones. Elevated levels of brightness in the BSE are indicative of higher Ta and lower Nb proportions in the crystal structure. In comparison to oscillatory zonation, crystals such as illustrated in Fig. 4*b* and *c* are still considered to be progressively zoned as there is an overall increase in the Ta proportions from core to rim, even though individual zones also show changes in brightness and therefore composition.

Oscillatory zonation is a common feature of columbite-group minerals and tapiolite and is generally the typical abundant zonation within a given pegmatite (e.g. Zhang *et al.*, 2004). However, oscillatory zonation, which is not as widespread in the Cape Cross–Uis pegmatite belt as progressive zonation, occurs equally in columbite-group minerals in both magmatic and altered zones. Oscillatory zonation occurs as repeating, alternating zones of different Ta and Nb compositions (Fig. 4*d*). As with progressively-zoned crystals, each specific zone may also show individual progressive zonation (Fig. 4*e*). The width of the zones in the oscillatory-zoned crystals may vary widely. In the case of Fig. 4*d*, zones at the core have an average width of several μm and then a larger 40 μm zone occurs, followed by extremely thin banded zones. Tapiolite shows the most prominent oscillatory zonation (Fig. 5). Thin, less than a micrometre in thickness, zones occur as banded layers that can either be concentric (Fig. 5a,*b*,*d*) or unidirectional (Fig. 5*c*) across the specific crystal face cross section. Zones similarly show varying widths with either slight changes in BSE brightness or more notable changes.

Abundant patchy zonation is typical of samples from altered zones. Patchy zonation may occur as resorption textures that have replaced primary grains/zones with later secondary undulating or irregularly shaped grains/rims (Fig. 4*a*,*d*,*e*,*f*). Patchy zonation has no particular affinity for grain cores or rims and is superimposed on either oscillatory or progressive zonation or both, giving the crystals complex zonation patterns (Fig. 4*b*,*e*,*f*). Patchy zonation generally shows the highest BSE brightness in all crystals, having the highest Ta contents, but may also occur as darker zones which appear to intrude a previously crystallised zone (Fig. 4*d*,*e*). Tapiolite occurs exclusively as patchy zones except in sample 3.1-2 (Fig. 5; all crystals are tapiolite in this figure).

Mineral compositions

Representative compositions of columbite-group minerals and tapiolite are given in Table 2. Columbite-group minerals display an extremely wide range of Ta_2O_5 and Nb_2O_5 contents from 1.8–82.3 and 1.8–72.9 wt.% respectively. FeO and MnO show similar broad ranges, 0.9–16.4 and 0.5–16.1 wt.%, respectively, however, most compositions are rich in Fe compared to Mn and show an average of 12.4 wt.% FeO and 5.1 wt.% MnO. SnO_2 and TiO_2 contents in general average ~0.9 wt.% but may exceed 4 wt.% in rare cases. Scandium, U, Ca and W show low to non-detectable levels that do not generally exceed 0.5 wt.%, however, it is notable that columbite-group minerals in the garnet–tourmaline pegmatites have WO_3 contents up to 4.0 wt.%. Anomalous elevated minor-element substitutions in columbite-group minerals are not unique to specific pegmatite groups, with the exception of W in garnet–tourmaline pegmatites. However, the columbite-(Fe) end-member, where present, shows the highest abundance of minor elements compared to the other end-members. The total atoms per formula unit (apfu) for columbite-group minerals and tapiolite cluster at 3 units for unaltered samples, however, greisenised samples show slightly elevated values of 3.1 apfu. Tapiolite shows less variation with respect to Ta_2O_5 and Nb_2O_5, having averages of 77.2 and 6.7 wt.% respectively. FeO contents cluster around 13.0 wt.% whereas MnO is much lower at an average of 1.0 wt.%. SnO_2 and TiO_2 are elevated compared to columbite-group minerals, commonly reaching 4.4 and 2.5 wt.% respectively. Magnesium, Ca, U, Sc and W were not detectable in tapiolite.

Intra-crystal tapiolite compositional variation

Sample 3.1-2 is the only one in the Cape Cross–Uis pegmatite belt that primary magmatic textures, such as concentric oscillatory-zoning in subhedral grains, were observed in individual tapiolite crystals (Fig. 5). However, multiple patchy zonation and resorption textures overprint oscillatory zonation. Individual crystals show the typical overall increase in Ta with respect to Nb, from the core outwards, regardless of alternating changes in Nb and Ta in oscillatory zonation (Fig. 5). Little change is observed in the Fe and Mn content through individual crystals (Fig. 5). The highest abundance of Ta (greatest BSE brightness) occurs in patchy zonation regardless of whether the patch is at the core or on the rim. Sn and Ti show that, on a single crystal-scale, as Ta is enriched, minor-element substitution decreases (Fig. 5*a*,*b*,*c*). There is also an apparent 'jump' in the decrease in Ti and Sn from the oscillatory zones to the patchy zones (Fig. 5*b*,*c*). These discrete tapiolite grains show that, on an individual crystal

https://doi.org/10.1180/mgm.2018.151 Published online by Cambridge University Press

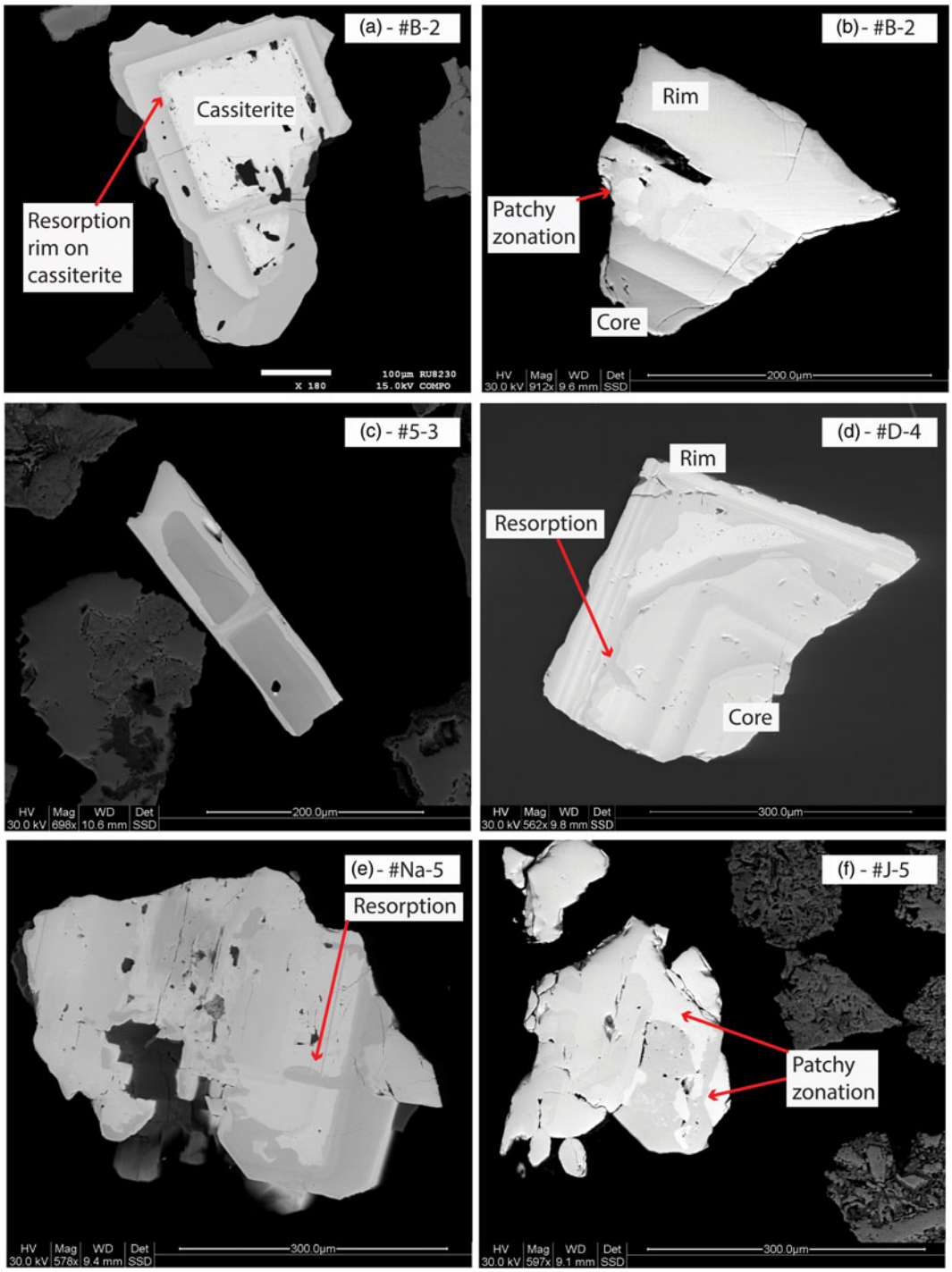

Fig. 4. Back-scattered electron images of various columbite-group minerals and cassiterite crystals. (*a*) Oscillatory-zoned columbite-group mineral enclosing a euhedral cassiterite grain showing a resorption texture along the margins of the cassiterite crystal. (*b*) Progressively-zoned columbite-group mineral with later-stage patchy zonation along the rim and centre zone. (*c*) Platy progressively-zoned columbite-group mineral. (*d*) Oscillatory-zoned columbite-group minerals with resorption textures in the large centre zones. (*e*) Multiple zonation of a columbite-group mineral showing later resorption of the rim and renewed oscillatory zonation. (*f*) Complexly-zoned columbite-group mineral showing patchy zonation.

scale and between the magmatic and late-stage patchy zonation, minor-element trends are similar to those of the samples seen in Fig. 6*a–d*. In addition, Fig. 5*a–c* shows that there is a decrease in the Nb contents from oscillatory to patchy zonation indicating an increase in the Ta/(Ta + Nb) ratios from different textural zones. Calculations of the Ta# in both oscillatory and patchy zonation show that patchy zonation has a Ta# 0.05 to 0.1 greater than oscillatory zonation.

Columbite-group minerals and tapiolite mineral composition

When the minor elements, Ti, Sn, Ca, Mg and W are plotted against Ta# for the entire dataset, weak hyperbolic trends are seen (Fig. 6*a–d*). Figure 6*a* displays this trend the best where early-crystallised (lower ranges of Ta#) tapiolite has high concentrations of Sn and Ti and later growth gradually becomes depleted in Sn and Ti with increasing Ta#. These trends are less defined for the entire dataset in Fig. 6*b–d*, however, by plotting each sample

https://doi.org/10.1180/mgm.2018.151 Published online by Cambridge University Press

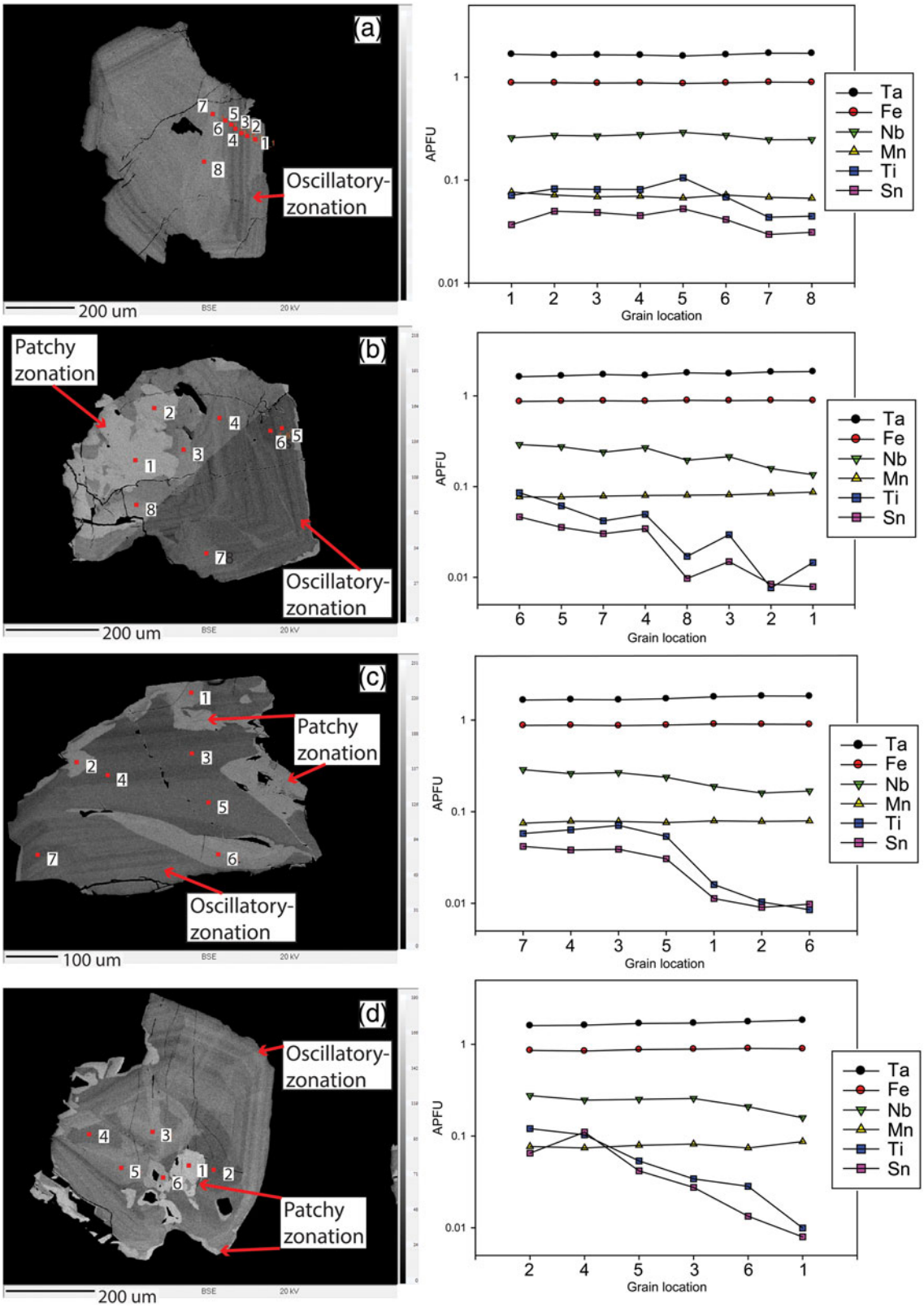

Fig. 5. Back-scattered electron images of individual tapiolite grains from sample 3.1-2 with their corresponding analyses of elements Ta, Fe, Nb, Mn, Ti and Sn at different points in the grains. Note that the numbers in the corresponding graphs (*x* axis) are ordered from darkest zones to lightest zones and not in ascending order. (*a*) Oscillatory-zone tapiolite crystal. (*b*) Twinned complexly-zoned tapiolite crystal. (*c-d*) Complexly-zoned tapiolite crystals.

separately this trend is clear and ubiquitous for all samples. Essentially there is an overall decrease in minor-element heterovalent substitution in columbite-group minerals and tapiolite with increasing Ta#. Tapiolite compositions are different compared to columbite-group minerals in that they have elevated Sn and Ti concentrations, which is why individual plots for tapiolite

https://doi.org/10.1180/mgm.2018.151 Published online by Cambridge University Press

Table 2. Representative compositions of columbite-group minerals and tapiolite from the Cape Cross–Uis pegmatite belt.

Peg. type	Grt–Tur	Li peg.	Ta–Nb–Sn									
Sample #	12-1	5-3	A-2	2-4	Na-5	Na-6	4-3	4-9	4-11	4-12	10-4	J-5
Mineral	FeC	FeT	FeC	FeC	FeC	FeC	FeT	FeC	FeC	FeC	FeC	FeC
Wt.%												
SnO_2	n.d.	0.09	0.19	0.03	0.14	0.74	0.24	0.15	0.17	0.17	0.75	0.22
MgO	0.40	0.08	n.d.	0.09	n.d.	n.d.	n.d.	n.d.	n.d.	n.d.	0.36	n.d.
Ta_2O_5	6.44	59.36	25.76	30.76	28.38	36.68	52.67	37.53	14.52	31.62	25.00	25.31
FeO	15.65	11.03	13.18	13.61	13.75	12.44	9.81	10.66	12.47	11.37	14.10	11.09
MnO	4.32	5.52	6.27	5.13	5.30	5.47	6.10	6.65	7.70	7.04	4.28	8.07
Nb_2O_5	67.85	22.67	54.98	50.23	52.70	43.99	27.90	44.15	64.72	49.26	52.20	55.13
TiO_2	2.16	0.34	0.60	0.70	0.39	0.88	0.85	0.19	0.56	0.33	2.32	0.44
Sc_2O_3	0.07	0.02	0.03	0.02	0.01	0.03	n.d.	0.03	n.d.	0.01	0.03	0.03
U_2O	n.d.	n.d.	n.d.	n.d.	n.d.	n.d.	n.d.	n.d.	n.d.	n.d.	n.d.	n.d.
CaO	n.d.	0.01	n.d.	n.d.	0.01	0.01	n.d.	n.d.	n.d.	0.02	n.d.	0.02
WO_3	3.93	n.d.	0.34	n.d.	n.d.	0.66	1.28	0.06	0.82	n.d.	1.46	0.77
Total	100.81	99.12	101.34	100.59	100.68	100.91	98.86	99.43	100.97	99.82	100.49	101.09
Atoms per formula unit												
Sn	n.d.	0.003	0.005	0.001	0.004	0.019	0.007	0.004	0.004	0.004	0.019	0.005
Mg	0.034	0.009	n.d.	0.009	n.d.	n.d.	n.d.	n.d.	n.d.	n.d.	0.033	n.d.
Ta	0.100	1.201	0.432	0.530	0.485	0.649	1.033	0.677	0.233	0.553	0.420	0.425
Fe	0.750	0.687	0.679	0.722	0.722	0.677	0.592	0.591	0.616	0.611	0.728	0.573
Mn	0.209	0.348	0.328	0.276	0.282	0.302	0.372	0.374	0.385	0.384	0.224	0.422
Nb	1.756	0.763	1.532	1.439	1.496	1.295	0.910	1.324	1.728	1.432	1.457	1.540
Ti	0.093	0.019	0.028	0.033	0.018	0.043	0.046	0.010	0.025	0.016	0.108	0.021
Sc	0.004	0.001	0.002	0.001	n.d.	0.002	n.d.	0.002	n.d.	0.001	0.001	0.002
U	n.d.	n.d.	n.d.	n.d.	n.d.	n.d.	n.d.	n.d.	n.d.	n.d.	n.d.	n.d.
Ca	n.d.	0.001	n.d.	n.d.	0.001	0.001	n.d.	n.d.	n.d.	0.001	n.d.	0.001
W	0.058	n.d.	0.005	n.d.	n.d.	0.011	0.024	0.001	0.013	n.d.	0.023	0.012
Total	3.004	3.031	3.010	3.011	3.007	2.999	2.985	2.982	3.004	3.002	3.012	3.002
Mn/(Mn + Fe)	0.054	0.612	0.220	0.269	0.245	0.334	0.532	0.338	0.119	0.279	0.224	0.216
Ta/(Ta + Nb)	0.218	0.336	0.325	0.276	0.281	0.308	0.386	0.387	0.385	0.386	0.235	0.424

Peg. type	Ta–Nb–Sn				Greisenised							Alb.
Sample #	D-4	T-4	3-3	3.2-1	5.1-1	3.1-2	G-4	B-2	W-3	x-1	M-2	4-4
Mineral	FeC	FeC	FeC	FeC	Tap	Tap	FeC	FeC	MnT	FeT	FeT	FeC
Wt.%												
SnO_2	0.23	0.20	0.20	0.39	3.29	4.35	0.22	0.23	0.06	n.d.	0.95	0.39
MgO	0.02	n.d.	0.01	0.26	0.02	n.d.	0.03	0.07	n.d.	n.d.	0.07	0.03
Ta_2O_5	17.57	33.03	31.97	27.71	73.12	75.53	24.82	25.54	63.08	52.73	57.55	26.38
FeO	13.69	11.25	12.25	13.38	14.77	13.03	14.98	12.73	4.77	9.37	11.87	12.29
MnO	5.63	7.44	6.08	5.16	0.69	0.75	6.21	6.40	11.48	7.34	4.31	7.58
Nb_2O_5	59.40	47.13	48.70	51.81	6.14	5.56	51.83	55.51	21.46	28.94	23.51	53.28
TiO_2	1.19	0.27	0.54	1.24	0.62	1.11	0.82	0.70	0.15	0.18	1.91	0.56
Sc_2O_3	0.02	0.04	n.d.	0.02	0.02	n.d.	n.d.	0.01	0.03	n.d.	0.09	n.d.
U_2O	n.d.	n.d.	n.d.	n.d.	n.d.	n.d.	n.d.	n.d.	n.d.	n.d.	n.d.	n.d.
CaO	n.d.	n.d.	0.02	n.d.	n.d.	n.d.	n.d.	n.d.	0.02	0.03	n.d.	n.d.
WO_3	2.43	0.34	0.24	0.62	n.d.	n.d.	0.11	0.18	n.d.	0.77	1.01	0.03
Total	100.17	99.69	100.00	100.59	98.66	100.89	99.02	101.36	101.05	99.36	101.26	100.55
Atoms per formula unit												
Sn	0.006	0.005	0.005	0.010	0.108	0.140	0.006	0.006	0.002	n.d.	0.027	0.010
Mg	0.002	n.d.	0.001	0.024	0.002	n.d.	0.003	0.006	n.d.	n.d.	0.008	0.003
Ta	0.289	0.584	0.559	0.471	1.630	1.658	0.427	0.427	1.268	1.030	1.119	0.448
Fe	0.692	0.611	0.659	0.699	1.012	0.880	0.793	0.654	0.295	0.563	0.710	0.642
Mn	0.288	0.409	0.331	0.273	0.048	0.051	0.333	0.333	0.719	0.447	0.261	0.401
Nb	1.624	1.385	1.415	1.464	0.228	0.203	1.483	1.542	0.717	0.940	0.760	1.504
Ti	0.054	0.013	0.026	0.058	0.038	0.068	0.039	0.032	0.009	0.010	0.102	0.026
Sc	0.001	0.002	n.d.	0.001	0.001	n.d.	n.d.	n.d.	0.002	n.d.	0.006	n.d.
U	n.d.	n.d.	n.d.	n.d.	n.d.	n.d.	n.d.	n.d.	n.d.	n.d.	n.d.	n.d.
Ca	n.d.	n.d.	0.001	n.d.	n.d.	n.d.	n.d.	n.d.	0.002	0.002	n.d.	n.d.
W	0.038	0.006	0.004	0.010	n.d.	n.d.	0.002	0.003	n.d.	0.014	0.019	n.d.
Total	2.994	3.016	3.000	3.010	3.067	3.000	3.086	3.003	3.012	3.006	3.012	3.035
Mn/(Mn + Fe)	0.151	0.297	0.283	0.243	0.878	0.891	0.224	0.217	0.639	0.523	0.596	0.229
Ta/(Ta + Nb)	0.294	0.401	0.334	0.281	0.045	0.055	0.296	0.337	0.709	0.442	0.269	0.384

FeC – columbite-(Fe); FeT – tantalite-(Fe); MnC – columbite-(Mn); MnT – tantalite-(Mn); Cas – cassiterite; Tap – tapiolite; n.d. – not detected; Alb – albitised.

and columbite-group minerals were used in Figs 6*a* and *b*. Furthermore, tapiolite data shows low contents of W, Mg and Ca compared to columbite-group minerals at lower Ta# values. This is an interesting observation as zonation patterns and Ta# show columbite-group minerals as an early-stage Ta–Nb oxide whereas tapiolite is mostly observed with patchy zonation,

https://doi.org/10.1180/mgm.2018.151 Published online by Cambridge University Press

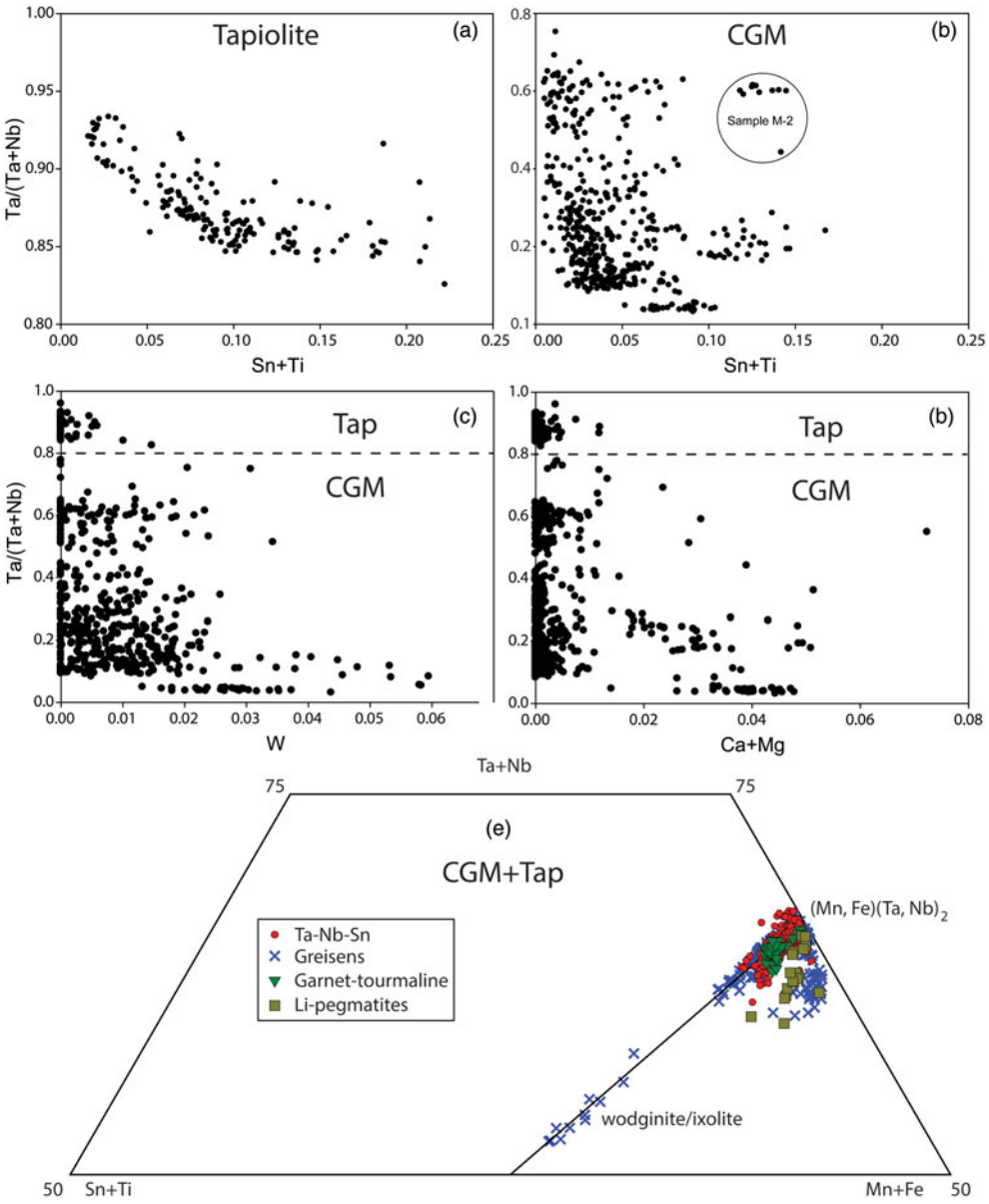

Fig. 6. Compositional variation plots of columbite-group minerals and tapiolite (data are in apfu; TAP = tapiolite; CGM = columbite-group minerals). (*a*) Sn and Ti values in tapiolite plotted against Ta# (Ta/(Ta + Nb)). (*b*) Sn and Ti values in columbite-group minerals plotted against Ta#. (*c*) W in both tapiolite and columbite-group minerals plotted against Ta#. (*d*) Ca and Mg in both tapiolite and columbite-group minerals plotted against Ta#. Each plot (*a*–*d*) groups elements of the same charge whereas tapiolite and columbite-group minerals are separated by a dashed line in plots *c* and *d*. (*e*) columbite-group minerals and tapiolite in a section of the (Sn + Ti) – (Mn + Fe) – (Ta + Nb) triangle. The diagonal line connecting to (Mn, Fe)(Ta, Nb)$_2$ indicates ideal substitution whereby the ratio of (Mn, Fe) to (Ta, Nb), or *A* site to *B* site, is 1:2. Points falling below this line indicate *B*-site deficiency in the crystal structure of columbite-group minerals, tapiolite or cassiterite.

appearing to be a late-stage Ta–Nb oxide. If we consider a transition from crystallising only columbite-group minerals, to columbite-group minerals and tapiolite, there is a marked increase in the Ti and Sn contents in newly crystallised tapiolite, followed by a repeat of the trend of decreasing minor-element heterovalent substitution with increasing Ta#. This 'jump' is absent for other minor elements, such as W, Ca and Mg, which remain at low concentrations in tapiolite (Fig. 6*c*,*d*).

Columbite-group minerals and tapiolite generally conform to an ideal Fe-Mn and Ta–Nb substitution with a 1:2 ratio of the *A* site to the *B* site (Fig. 6*e*). Ideal substitution is shown by the (Mn, Fe) = 2(Ta, Nb) tie line in Fig. 6*e*. Deviations from the ideal substitution are found dominantly in columbite-group minerals and tapiolite from greisen samples where there is a notable deficiency in the *B*-site cations, Ta and Nb, as these samples plot below the ideal substitution line (Fig. 6*e*). The columbite-group minerals in Li pegmatites show a similar distinct depletion in the *B*-site cations, Ta and Nb, being Fe-Mn enriched relative to Ta and Nb.

Columbite-group mineral compositions in most samples plot in a linear fashion from the columbite-(Fe) field into the tantalite-(Fe) field with increasing Ta# and little or no change in the Mn# in the columbite quadrilateral (Fig. 7*a*–*c*). Compositions terminate against the tapiolite gap described in Černý *et al.* (1992*b*). The tapiolite gap is a compositional gap between the tetragonal tapiolite field and orthorhombic columbite-group mineral field (Fig. 7) where it is not uncommon for some data to plot on or near the boundary of the field. Some samples show that co-occurring

https://doi.org/10.1180/mgm.2018.151 Published online by Cambridge University Press

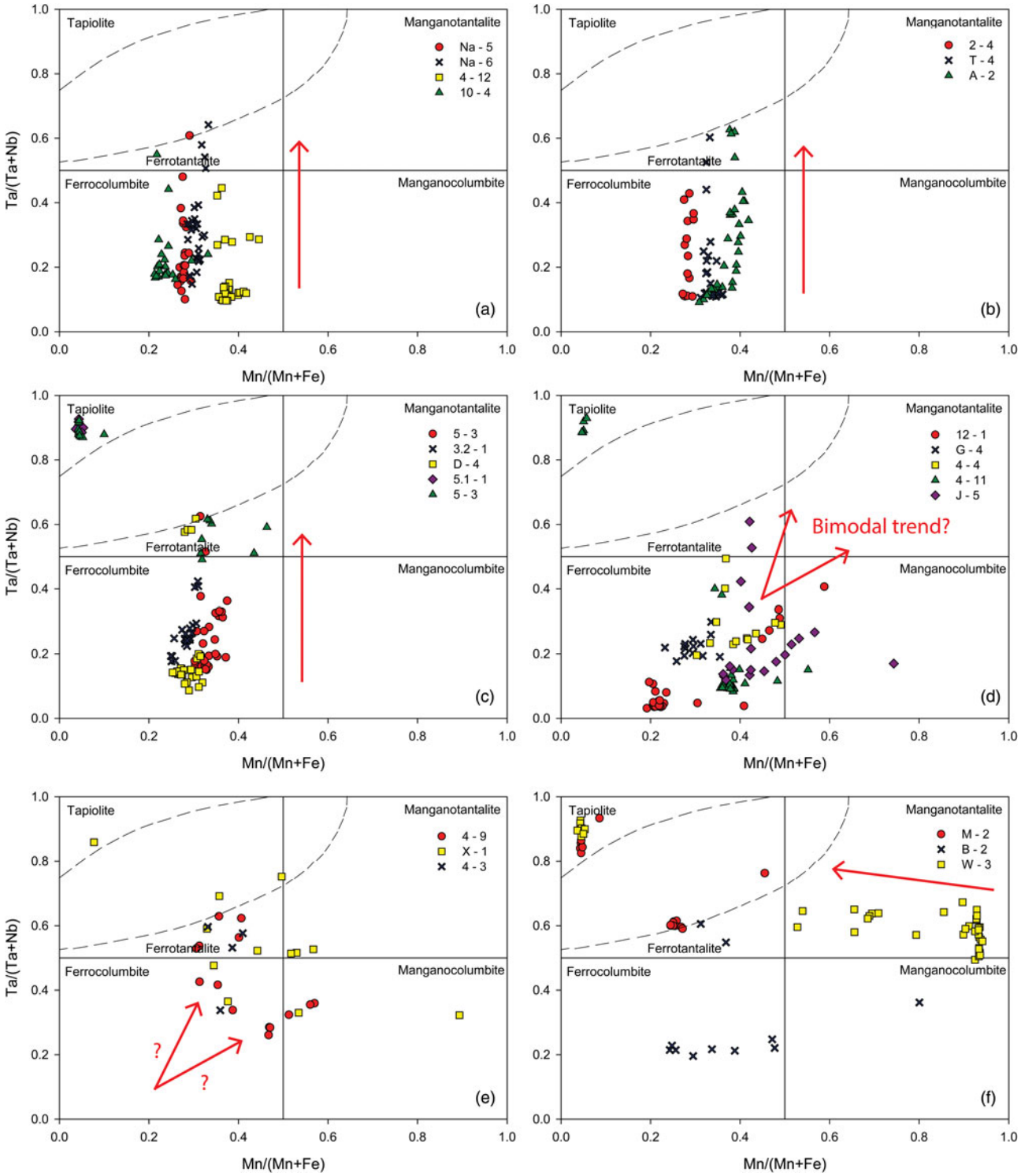

Fig. 7. Columbite-group minerals and tapiolite compositions for individual samples in the columbite quadrilateral (ferro and mangano used as prefixes for the suffixes -(Fe) and -(Mn), respectively). The samples are grouped roughly according to the trend they display which is shown by the red arrows in each plot. (*a–c*) Typical trends subparallel to the Ta/(Ta + Nb) axis, defined by increasing Ta# with little variation in the Mn#. (*d*) Apparent bimodal fractionation trends in samples J-5, 4-4 and 4-11. Sample 12-1 shows a concomitant trend of equal increases in the Ta# and Mn# whereas sample G-4 clusters in the columbite-(Fe) field with no discernible trend. (*e,f*) Columbite-group minerals and tapiolite that display uncharacteristic behaviour. Sample 4-9 potentially shows a bimodal trend with missing data in the columbite-(Fe) field (indicated by red arrows). Sample W-3 potentially shows a trend of decreasing Mn# with slight increases in the Ta# (indicated by the red arrow in *f*). Other data is scattered. The tapiolite immiscibility gap is shown in the figures as dashed lines in the tantalite-(Fe) field (top left).

tapiolite is present to give a complete trend: columbite-(Fe) → tantalite-(Fe) → tantalite-(Fe) + tapiolite (Fig. 7*c*). As Ta# is an indication of fractionation, these samples that have co-occurring tapiolite are the most fractionated. Data points that plot in the tapiolite field are notably Fe rich and co-occurring tantalite-(Fe) and tapiolite show moderate gradient (1:1) lines linking the two

https://doi.org/10.1180/mgm.2018.151 Published online by Cambridge University Press

Ta–Nb phases. Figure 7*d* shows that some samples have columbite-group minerals which appear to have a bimodal fractionation trend, with initial compositions clustering in the columbite-(Fe) field and then proceeding both towards the tantalite-(Fe) field with increasing Ta# and towards the columbite-(Mn) field with equal increases in Ta# and Mn#. Sample 4-9, Fig. 7*e*, also possibly shows this bimodal trend. It is also notable in Fig. 7*d*, Sample 12-1, that the columbite-group minerals of the garnet–tourmaline pegmatite have the lowest Ta# in the dataset and show a distinct concomitant trend, starting in the columbite-(Fe) field with equal increases in Ta# and Mn# into the columbite-(Mn) field. Other samples (Fig. 7*e*,*f*) show a scattering of data where no discernible trends are observed, with the exception of sample W-3 (Fig. 7*f*) that possibly evolves from the tantalite-(Mn) field towards the tantalite-(Fe) field. It appears that data with the lowest Ta# in sample W-3 have the highest Mn#, subsequent data being more scattered at higher Ta# and lower Mn#.

On a regional pegmatite belt scale when comparing data from all samples, columbite-group minerals show an overall trend in the columbite-group minerals quadrilateral subparallel to the Ta/(Ta + Nb) axis due to increasing Ta# with little change in the Mn# (Fig. 8). Columbite-group minerals and tapiolite from greisen samples display the highest Ta# in the dataset with most tapiolite occurring in greisenised samples (Fig. 8). Similarly, only greisens show compositions that plot in the tantalite-(Mn) field. Lithium pegmatites also show high Ta# plotting well within the tantalite-(Fe) and tapiolite field with only one datum plotting in the columbite-(Fe) field. Nb–Ta–Sn pegmatite types show a wide variety of compositions, having intermediate Ta# and Mn# values compared to the other pegmatite types and altered zones.

Cassiterite

Occurrence and internal structure

In the Cape Cross–Uis pegmatite belt cassiterite has been observed in fewer pegmatites than columbite-group minerals, although it has a greater overall abundance in terms of tonnage. The Uis swarm hosts most of the cassiterite in the area possibly reflecting the larger dimensions of the pegmatites in the swarm and the increased degree of greisenisation compared to other swarms (Fuchsloch *et al.*, 2018). Cassiterite generally occurs as black anhedral- to- subhedral grains ranging from rectangular 5 cm x 1 cm crystals to fine-grained 0.5–1 mm grains in albitised zones. Rare euhedral, bypyramidal and sub-transparent crystals up to a size of 1.3 cm along the *a* axis also occur. Local artisanal miners have also identified 'red tin' which has a red hue and rusty texture and occurs mostly as 1–2 mm equidimensional grains.

Microscopically cassiterite is generally homogeneous and rarely shows any zonation on BSE imagery (Fig. 4*a*). Cassiterite occasionally co-occurs in association with columbite-group minerals in unaltered magmatic assemblages either adjacent to or as individual crystals. In altered zones, columbite-group minerals are observed as epitaxial overgrowths around cassiterite crystals where the rims of the cassiterite show resorption textures (Fig. 4*a*). A feature in the Uis swarm is the occurrence of oscillatory-zoned, columbite-group mineral inclusions within cassiterite. Some inclusions show resorption textures but there is no indication of the columbite-group minerals having been derived from exsolution in cassiterite.

Cassiterite mineral composition

Cassiterite shows little to moderate variation in its composition, with most crystals consisting of almost pure SnO_2 (Table 3). Some homogenous grains with no associated columbite-group mineral inclusions exhibit elevated Ta_2O_5 contents of ~5 wt.% (Table 3; Sample Na-5 and J-5). Generally, it is the cassiterite from greisens that show slightly higher Ta_2O_5 contents between 1 and 3 wt.%. No distinguishable differences were observed between cassiterite from different pegmatite groups except for the absence of Ta_2O_5 in cassiterite from the Li pegmatites. Although cassiterite typically contains 0.16–1.83 wt.% FeO, there is no specific variation between pegmatite groups. Nb_2O_5 contents are generally <0.5 wt.%, however, some greisen samples contain cassiterite with Nb_2O_5 contents >2 wt.%. Mn is notably present in low concentrations together with Sc, U, W, Ca and Ti.

In a (Ta,Nb) – (Sn,Ti) – (Mn,Fe) plot, cassiterite compositions mostly show ideal compositional variations along a line defined by the substitution reaction $(Fe, Mn)^{2+} + 2(Ta, Nb)^{5+} = 3(Sn,Ti)^{4+}$ (Fig. 9*a*). This line indicates that the proportions of Fe–Mn and Ta–Nb conform to the ideal ratio of 1:2. However, cassiterite from Li pegmatites plot below the ideal substitution line indicating $(Ta, Nb)^{5+}$ depletion with respect to $(Fe, Mn)^{2+}$ and show the lowest Ta#. Some cassiterite from greisen samples also plot below the ideal substitution line whereas none of the compositions plot significantly above it. The Ta# of cassiterite in the dataset shows a wide variety of values whereas the Mn# is mostly below 0.2 (Fig. 9*b*). No specific trend is observed in a plot of Ta# *vs*. Mn#, however, data with Ta# >0.6 appear to show slightly higher Mn# values.

Discussion

The approach we take in this study is to characterise three main factors that occur during the paragenesis of the pegmatites and Ta–Nb and Sn oxides: (1) the minor-element evolution in Ta–Nb oxides; (2) the fractional crystallisation evolution; and (3) the potential of a phase transition from a magmatic to an exsolved pegmatitic aqueous fluid.

Minor-element evolution

The fractionation of Ta from Nb is well established in experimental work (Linnen and Keppler, 1997; Linnen, 1998) which found that in silicate melts, Ta-bearing phases are more soluble than their Nb-bearing counterparts (Ta# increases during fractionation). Minor-element heterovalent substitution in Ta–Nb oxides is greatest in the early stages of pegmatite crystallisation and decreases with fractionation into the late stages of crystallisation (Fig. 6*a*–*d*). Although similar trends have been recorded in the Varuträsk pegmatite, Sweden (Černý *et al.*, 2004), an explanation of the phenomenon is not clear. Ercit *et al.* (1995) questioned whether this evolutionary compositional trend is crystal-chemical or geochemical in origin by comparing the minor-element trend to the state of order in the crystal structure of columbite-group minerals, i.e. do the mechanisms of hetrovalent substitution induce cation disorder or do columbite-group minerals with high contents of minor elements form early in the crystallisation history of the pegmatite when disordered states are more stable, allowing higher levels of minor-element substitution? A possible explanation, favouring the crystal-chemical origin, is that as other phases in the magma chamber began to stabilise, the minor elements favoured these newly stabilised minerals and therefore their abundances in columbite-group minerals and tapiolite decreased during fractionation. This hypothesis is important for Fe–Mn fractionation trends in columbite-group minerals as some authors suggest (Van Lichtervelde *et al.*,

https://doi.org/10.1180/mgm.2018.151 Published online by Cambridge University Press

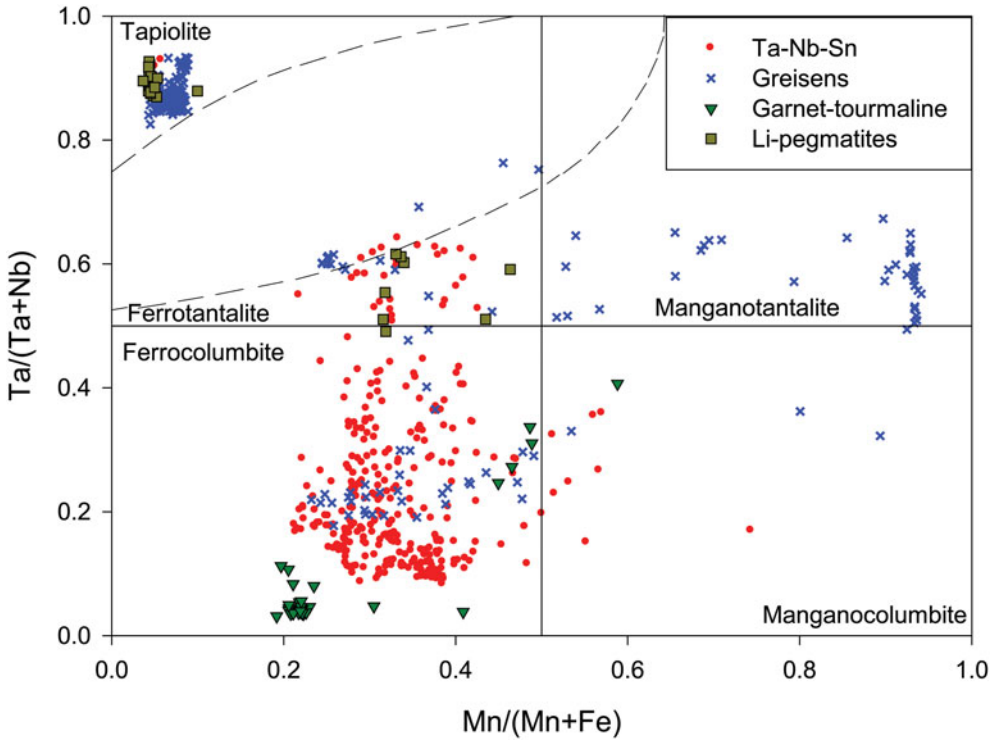

Fig. 8. Combined compositional data of columbite-group minerals and tapiolite from all samples in the Cape Cross–Uis pegmatite belt. Samples are plotted based on the pegmatite group to which they belong (Table 1) and whether a sample is an altered greisenised zone (blue crosses). Ferro and mangano used as prefixes for the suffixes -(Fe) and -(Mn), respectively.

2007) that co-existing phases competing for Mn, also control the fractionation of Fe from Mn.

Tapiolite is considered to form at late stages in pegmatites (Černý *et al.*, 1992*b*). This is supported by abundant tapiolite being primarily found in greisenised zones of the pegmatites of the Cape Cross–Uis pegmatite belt (Fig. 8). Furthermore, and with the exception of some grains in sample 3.1-2, tapiolite exclusively has patchy zonation within pegmatites (Fig. 5). Co-occurring tapiolite and columbite-group minerals generally represent a composition that plots within the tapiolite gap giving rise to the pair of mineral phases, however, tapiolite shows much higher contents of Sn and Ti at a low Ta# (Fig. 6*a*; Černý *et al.*, 1992*b*). If the crystallisation sequence is considered to transfer from columbite-group minerals to columbite-group minerals and tapiolite, then there is an observed increase in the Sn and Ti contents in tapiolite compared to columbite-group minerals. Tapiolite has a tetragonal crystal structure and therefore a greater affinity for Sn and Ti which can account for the increase in concentration of these minor elements in tapiolite (Neiva, 1996). Tapiolite repeats the same trend for Sn and Ti as seen in columbite-group minerals of decreasing minor-element substitution with increasing Ta# and fractionation. The abundance of cassiterite within the greisenised zones suggests that cassiterite competed for Sn and Ti, which favoured cassiterite as the solubility of cassiterite decreased and cassiterite stabilised.

Tapiolite shows no change in concentration compared to columbite-group minerals when other minor elements, Ca, Mg and W are compared to Sn and Ti. This is difficult to account for, considering the limited research of partition coefficients of specific elements into the tapiolite crystal structure. In essence, tapiolite might have no affinity for these minor elements or perhaps they had already been depleted in the crystallising liquid at the late-stages of crystallisation. In addition, these elements may have had a low activity during this phase of crystallisation if tapiolite is considered to crystallise from an exsolved aqueous fluid phase that did not preferentially partition Ca, Mg and W. Apart from the Ca, Mg and W concentrations in tapiolite, we suggest that minor-element trends in columbite-group minerals and tapiolite are governed by competing mineral phases.

Fractional crystallisation evolution of pegmatitic melts

Many authors have debated the controlling factors that lead to the fractionation of Fe from Mn or the lack of fractionation of Fe from Mn in Ta–Nb and Sn oxides. For example, Mulja *et al.* (1996), Raimbault (1998), Van Lichtervelde *et al.* (2007) and Beurlen *et al.* (2008) suggest that co-existing phases competing with columbite-group minerals for Fe in the pegmatites deplete Fe in columbite-group minerals during fractionation leading to Mn-rich end-members. Van Lichtervelde *et al.* (2007) elaborate on this and show late-stage Ta–Nb oxides become progressively richer in Fe during fractionation and suggest that the natural fractionation progression of Ta–Nb oxides is one of Fe enrichment when competing mineral phases are absent. The depletion of Fe in columbite-group minerals is typical of the lepidolite-type pegmatites and typically precedes fractionation of Ta from Nb. Other authors (Černý, 1992*b*; Tindle and Breaks, 2000; Černý *et al.*, 2004; Wise *et al.*, 2012) suggest that an increased alkali-fluoride activity promotes the extreme Fe–Mn fractionation before the onset of Ta enrichment, instead of a competing mineral phase control.

It is difficult to add to this debate based on the current study as the dominant pegmatite fractionation trend in Ta–Nb and Sn

https://doi.org/10.1180/mgm.2018.151 Published online by Cambridge University Press

Table 3. Representative compositions of cassiterite from the Cape Cross–Uis pegmatite belt.

Peg. type	Li peg	Ta–Nb–Sn						Greisenised				
Sample #	5-3	Na-5	J-5	A-2	T-4	3-3	3.2-1	B-2	X-1	M-2	G-4	3.1-2
Wt.%												
SnO_2	98.21	94.57	93.25	100.69	98.91	99.51	97.93	99.27	94.08	97.89	95.26	94.24
MgO	0.07	0.11	0.08	0.12	0.08	0.11	0.09	0.09	0.09	0.10	0.08	n.d.
Ta_2O_5	n.d.	4.18	5.75	0.34	0.18	0.85	1.74	0.26	2.66	1.15	n.d.	3.07
FeO	1.05	0.91	0.90	0.11	0.12	0.16	0.43	0.17	0.82	0.19	1.83	0.88
MnO	0.04	n.d.	0.08	0.02	0.01	0.02	0.01	n.d.	0.05	0.01	0.04	n.d.
Nb_2O_5	0.28	1.20	0.25	0.04	0.63	0.22	0.59	0.70	2.00	0.10	2.40	1.76
TiO_2	0.01	0.08	n.d.	0.13	0.03	0.07	0.26	0.16	0.09	0.25	0.30	0.07
Sc_2O_3	n.d.	n.d.	n.d.	n.d.	n.d.	n.d.	n.d.	n.d.	n.d.	n.d.	n.d.	n.d.
U_2O	n.d.	n.d.	n.d.	n.d.	n.d.	n.d.	n.d.	n.d.	n.d.	n.d.	n.d.	n.d.
CaO	n.d.	0.50	0.51	0.52	0.51	0.54	0.49	0.53	0.50	0.52	n.d.	n.d.
WO_3	n.d.	0.37	n.d.	n.d.	n.d.	n.d.	n.d.	n.d.	0.02	n.d.	n.d.	n.d.
Total	99.66	101.91	100.82	101.97	100.47	101.48	101.54	101.18	100.31	100.20	99.90	100.02
Atoms per formula unit												
Sn	2.949	2.777	2.787	2.952	2.938	2.933	2.880	2.924	2.791	2.920	2.820	2.816
Mg	0.008	0.012	0.009	0.013	0.009	0.013	0.010	0.010	0.011	0.011	0.009	n.d.
Ta	n.d.	0.084	0.117	0.007	0.004	0.017	0.035	0.005	0.054	0.023	n.d.	0.063
Fe	0.066	0.056	0.056	0.007	0.007	0.010	0.027	0.010	0.051	0.012	0.114	0.055
Mn	0.003	n.d.	0.005	0.001	0.001	0.001	0.001	n.d.	0.003	0.001	0.003	n.d.
Nb	0.010	0.040	0.008	0.001	0.021	0.007	0.020	0.024	0.067	0.003	0.081	0.060
Ti	0.001	0.004	n.d.	0.007	0.002	0.004	0.014	0.009	0.005	0.014	0.017	0.004
Sc	n.d.	n.d.	n.d.	n.d.	n.d.	n.d.	n.d.	n.d.	n.d.	n.d.	n.d.	n.d.
U	n.d.	n.d.	n.d.	n.d.	n.d.	n.d.	n.d.	n.d.	n.d.	n.d.	n.d.	n.d.
Ca	n.d.	0.039	0.041	0.041	0.041	0.043	0.039	0.042	0.040	0.042	n.d.	n.d.
W	n.d.	0.007	n.d.	n.d.	n.d.	n.d.	n.d.	n.d.	n.d.	n.d.	n.d.	n.d.
Total	3.036	3.019	3.024	3.029	3.023	3.027	3.024	3.024	3.022	3.026	3.042	2.997
Mn/(Mn + Fe)	0.037		0.086	0.130	0.077	0.099	0.019		0.055	0.041	0.022	
Ta/(Ta + Nb)		0.677	0.934	0.840	0.149	0.700	0.640	0.181	0.445	0.880		0.512

n.d. – not detected

oxides is controlled by increasing Ta# (Figs 7, 8 and 9) where Ta is enriched relative to Nb and there is little fractionation between Fe and Mn, similar to pegmatites observed in Mulja *et al.* (1996), Tindle and Breaks (2000) and Beurlen *et al.* (2008). Essentially the pegmatites in the Cape Cross–Uis pegmatite belt show both a lack of F-bearing phases and minerals that may compete for Mn, both of which may cause the observed fractionation trend. Evaluating the outliers that do not conform to the typical trend may provide some insight (Fig. 7*d–f*). It may be possible that sample W-3 (late-stage greisenised sample; Fig. 7*f*) follows a similar fractionation trend to the ones observed by Van Lichtervelde *et al.* (2007) in that Fe enrichment is the natural progression of fractionation in columbite-group minerals. The garnet–tourmaline pegmatite type also shows a concomitant fractionation trend in the Cape Cross–Uis pegmatite belt (Fig. 7*d*) similar to that noted in the pegmatites of the Preissac-Lacorne batholith, Canada, by Mulja *et al.* (1996), where garnet occurrence in pegmatites is a controlling factor in Fe–Mn fractionation. This favours a co-existing mineral phase argument instead of the amount of alkali-fluoride activity. However, this trend might also be attributed to the garnet–tourmaline pegmatites having a slight NYF affinity (Fuchsloch *et al.*, 2018) and, although not measured, might potentially have higher abundances of F (Wise *et al.*, 2012). Other bimodal trends and scattered data are more difficult to account for (Fig. 7*d–f*). Scattered data have been attributed to disequilibrium crystallisation in Ta–Nb and Sn oxides from other pegmatites (Splide and Shearer, 1992; London, 2008) and the changes in thickness of oscillatory zones observed in columbite-group minerals and tapiolite (Figs 4*d*, 5*b,c*) support disequilibrium crystallisation (Lahti, 1987). Bimodal fractionation trends may likewise be a consequence of disequilibrium or *in situ* crystallisation, however, to our knowledge, no other similar bimodal trends have been presented in the literature. Local saturation in a boundary layer can be discredited as the cause of bimodal trends as the samples and pegmatites are homogenous and not zoned mineralogically (e.g. Gonzàlez *et al.*, 2017). Perhaps these samples reflect a period in the crystallisation history of the pegmatites where Mn-competing phases stabilised in the melt thus changing the trend of newly crystallised columbite-group minerals.

Minor-element substitution trends in columbite-group minerals and tapiolite favour a co-existing mineral phase argument, if one agrees that minor-element substitution in Ta–Nb oxides induces mineral structural disorder, however, Ercit *et al.* (1995) stresses that a broader range of Ta–Nb-bearing rock types requires investigation. Whatever the ultimate explanation as to the controlling factors of Fe–Mn fractionation, the pegmatites of the Cape Cross–Uis pegmatite belt have a beryl-to-spodumene Ta–Nb-oxide pegmatite signature (Černý, 1992*b*) and a typical Ta# increase during fractionation with little change in the Mn#.

Magmatic vs. exsolved aqueous fluid crystallisation

There is a general consensus amongst authors that patchy zonation in columbite-group minerals and tapiolite (Figs 4, 5) is the result of re-equilibration of columbite-group minerals and tapiolite with later fluids, whether they were magmatic (Tindle and Breaks, 2000; Van Lichtervelde *et al.*, 2007, 2008), metamorphic (Černý *et al.*, 1992*a*) or exsolved aqueous fluid (Novák and Černý, 1998; Zhang *et al.*, 2004; Alfonso and Melgarejo, 2008; Ashworth, 2013; Balloured *et al.*, 2016). Similarly,

https://doi.org/10.1180/mgm.2018.151 Published online by Cambridge University Press

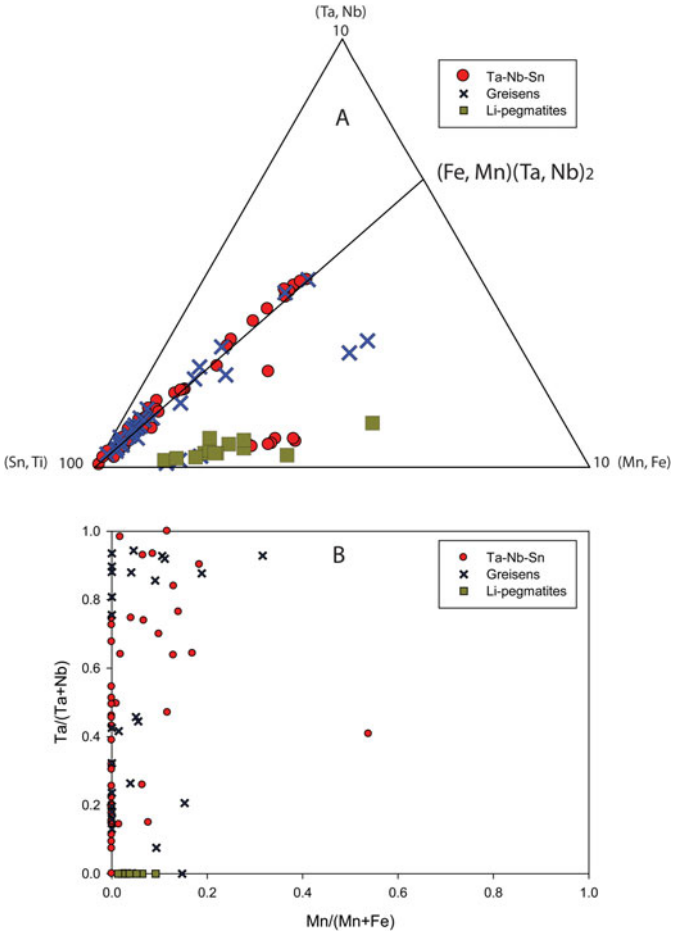

Fig. 9. Compositional characteristics and trends in cassiterite from the Cape Cross–Uis pegmatite belt. (*a*) (Sn,Ti) – (Ta,Nb) – (Fe,Mn) triangular plot showing the solid solution with columbite-group minerals (ideally with rutile structured tapiolite). The line marked $(Fe,Mn)(Ta,Nb)_2$ represents the ideal substitution. This graph shows the detail of the bottom left portion of the triangular diagram where (Sn, Ti) = 100% and (Ta,Nb) and (Mn,Fe) up to 10%. (*b*) Cassiterite compositions plotted in the columbite quadrilateral

oscillatory and progressive zoning are indicative of a magmatic regime (see discussions in Lahti, 1987 and Van Lichtervelde *et al.*, 2007).

The underlying principle surrounding the debate is not if a pegmatitic magma will exsolve an aqueous fluid but instead is directed at the partition coefficients of Ta and Nb into the aqueous fluid. Many authors have shown that the presence of an aqueous fluid being exsolved from the pegmatitic magma in the late stages of petrogenesis is probable (London, 2008). For example, the muscovite chemistry of greisens in the Tanco pegmatite, Canada, show characteristics of crystallisation from an aqueous fluid (Van Lichtervelde *et al.*, 2008). In essence, are Ta–Nb-bearing phases crystallised from a highly fractioned magma (Van Lichtervelde *et al.*, 2008) with or without a co-existing aqueous fluid or are they crystallised directly from the aqueous fluid itself? In the case of aqueous fluid crystallisation, Ta and Nb partition preferentially into the aqueous fluid, causing saturation of Ta and Nb and subsequently crystallising Ta–Nb-bearing phases (Alfonso and Melgarejo, 2008). In either case, the authors on both sides of the debate present evidence for and against crystallisation from a magmatic phase. For example, Van Lichtervelde *et al.* (2008) suggests, based on the experimental evidence of Chevychelov *et al.* (2005), that a late, rare-metal and flux-enriched magma may produce metasomatic features such as patchy zonation whereas other authors (Zhang *et al.*, 2004; Alfonso and Melgarejo, 2008) use patchy zonation as evidence of crystallisation from an aqueous fluid as Ta–Nb oxides are synchronous with greisenisation and other late-stage fluid-alteration products.

Chevychelov *et al.* (2005) showed that the partition coefficients of Ta and Nb into a co-existing aqueous fluid were very low (0.002–0.080 and 0.005–0.080, respectively). Van Lichtervelde *et al.* (2007, 2008) argue, based on this study, that an aqueous fluid could not transport significant quantities of Ta and Nb and subsequently crystallise Ta–Nb-bearing phases during alteration of K-feldspars to muscovite in greisens. However, the experimental study of Chevychelov *et al.* (2005) was based on fluoride aqueous fluids only and at temperatures exceeding 900°C. More probable pegmatitic crystallisation temperatures for the Cape Cross–Uis pegmatite belt, shown by Ashworth (2013), are between 450°C and 550°C with hypersaline and aqueo-carbonic fluid compositions. In addition, the experimental study shows that decreasing temperatures cause significant increases in the partition coefficient of Ta in an aqueous fluid whereas the Nb partition coefficient shows negligible changes with decreasing temperatures. Perhaps at pegmatitic conditions, the Ta partition coefficients for an aqueous fluid may be higher than the Nb partition coefficient.

A suitable example from this research is the Ta# variation between patchy zonation and oscillatory zonation. Figure 5 shows that patchy zonation has lower Nb contents than Ta compared to oscillatory zonation indicating patchy zonation has a higher Ta#. If the partition coefficient of Ta into an aqueous fluid increases with decreasing temperature and the Nb partition coefficient remains relatively unchanged, it can therefore be inferred that patchy zonation, at pegmatitic temperatures, has a higher Ta# if crystallised from an aqueous fluid. However, Chevychelov *et al.* (2005) only extrapolate their data for Ta to lower temperatures of 600°C and do not extrapolate data for Nb. As this is only an extrapolation and in light of the limited experimental research, only hypothetical situations may be discussed. For example, Van Lichtervelde *et al.* (2007) found that Ta# in both patchy and co-existing oscillatory/progressive zonation is roughly constant for both types of zonation, therefore, as Nb and Ta have different partition coefficients (Chevychelov *et al.*, 2005) for an aqueous fluid phase, crystallised from a magmatic phase.

Some of the data for columbite-group minerals, tapiolite and cassiterite show non-stoichiometric values (Figs 6*e*, 9*a*) in terms of the ratio of *A*-site and *B*-site cations. It is notable that these minerals occur ubiquitously, expect for sample 5-3, in greisens and are depleted in Ta and Nb (*B* site) relative to Fe and Mn (*A* site). As Ercit *et al.* (1995) points out, this may be geochemically or crystal-chemically controlled. The stoichiometry may be controlled by the state of order of the crystals, being different in the early- and late-stages of Ta–Nb–Sn-oxide crystallisation. Another hypothesis is that the Ta and Nb in magmatically crystallised minerals are remobilised preferentially over Fe and Mn during the greisenisation process by either a highly differentiated magma in the late-stages of crystallisation or an exsolved pegmatitic hydrothermal fluid. This would account for Ta–Nb–Sn oxides in greisens having a *B*-site deficiency. However, the fluid that might cause remobilisation is still debatable and comes down to the understudied partition coefficients of these elements at pegmatitic conditions.

https://doi.org/10.1180/mgm.2018.151 Published online by Cambridge University Press

The characteristics of zonation and associated minerals is important when considering their co-crystallising nature. Minor elements show that cassiterite competes with Ta–Nb-bearing phases for Sn and Ti (Fig. 6*a*). Cassiterite is known to crystallise preferentially from an aqueous phase with partition coefficients of Sn into an aqueous fluid being high, examples being cassiterite-bearing quartz veins (e.g. Kovalenko *et al.*, 1986). Cassiterite, tapiolite and columbite-group minerals show an intimate mineralogical relationship, specifically in synchronous alteration zones such as greisens (Fig. 4*a*). It would therefore be plausible that the crystallising medium of cassiterite is concomitant to the fluid or magma crystallising Ta–Nb-bearing phases. As abundant cassiterite is suggested to crystallise from an aqueous fluid specifically in greisen zones (Fuchsloch *et al.*, 2018), it would be incongruent for the Ta–Nb-bearing phases to be crystallising synchronously from another phase such as a highly fractionated magma simultaneously.

Other evidence that would suggest that Ta and Nb partition preferentially into an aqueous fluid phase is the presence of high concentrations of Ta and Nb in metasomatic, tourmalinised host-rock schist contact zones in pegmatites. Fuchsloch (2018) and Fuchsloch *et al.* (2018) report data of host-rock schists in contact with pegmatites, that show a high degree of tourmalinisation and metasomatism, which have significantly elevated values of Sn, Ta and Nb (Fig. 10). Out of six metasomatic contact schists, five are above that of general host-rock schists that show no metasomatic features and occur some distance away from pegmatites. Furthermore, the increases in the Ta concentrations of the metasomatic contacts show a correlation with increases in Sn and Nb indicating these elements are co-genetic with Ta (Fig. 10). Only one metasomatic schist showed lower Sn concentrations coupled with high Ta concentrations. In one case, the Ta content of the metasomatic schist is two orders of magnitude higher than schists which do not show metasomatic features (250 ppm Ta compared to 1–2 ppm, respectively). This metasomatic schist sample is so enriched in Ta it is comparable to economically mineralised pegmatites.

If the physical mobility of the crystallising fluid, magmatic or aqueous, is considered, it would be more reasonable for an aqueous fluid to transport these elements and enrich country-rock contacts. This is particularly evident in zoned pegmatite bodies which crystallise inwards, essentially trapping the highly fractionated magma in the late stages of petrogenesis within itself. An aqueous fluid is likely to percolate through to country rocks which London (2008) suggests is the cause of massive tourmalinisation of country rocks as these fluids also carry boron.

In summary, until repeatable results can be obtained on the partition coefficients of Ta and Nb in various aqueous fluids at pegmatitic conditions, no factual hypothesis may be derived with respect to crystallisation of Ta–Nb-bearing phases in the late-stages of pegmatitic petrogenesis. Although some studies have begun to tackle this problem (e.g. Smirnov *et al.*, 2012), these investigations did not measure the Ta contents of the aqueous fluid and the Ta-bearing experiments did not reach equilibrium. Moreover, country-rock contacts were not a detailed focus of Fuchsloch (2018) and therefore the dataset is limited to few samples which have not been studied in detail, for example, which minerals contain the Ta, Nb and Sn in metasomatised country rocks? A detailed investigation should be carried out on these country rocks in future which should involve a systematic sampling programme, whole-rock geochemistry, mineral chemistry and petrography. From an initial perspective, the Ta, Nb and Sn contents of country rock contacts and the intimate relationship between cassiterite, columbite-group minerals and tapiolite in greisen zones in pegmatites of the Cape Cross–Uis pegmatite belt is more consistent with crystallisation from an aqueous fluid during greisenisation.

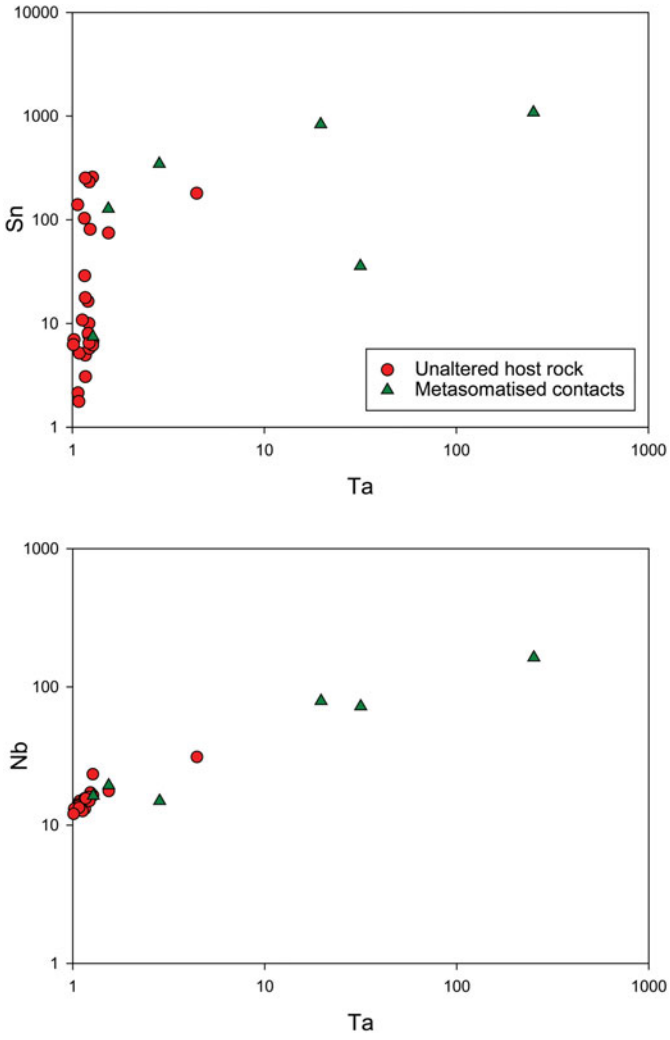

Fig. 10. Country-rock whole-rock data showing the Ta plotted against Sn and Nb in the upper and lower graphs respectively. The rock types include general host rocks which show no alteration and occur at variable distances to pegmatites and metasomatised, tourmalinised host-rock contacts with pegmatites. Plots are given in logarithmic scales due to orders of magnitude differences between the data.

Regional aspects

Fuchsloch *et al.* (2018) showed that the different pegmatite types in the Cape Cross–Uis pegmatite belt are not only different in terms of mineralogy and host-rock but also have different fractionation signatures and degrees of fractionation. The garnet–tourmaline pegmatites show primitive fractionation signatures whereas the Nb–Ta–Sn type show intermediate fractionation signatures, while the Li pegmatites show evolved fractionation signatures. The authors showed that the spatial distribution of the different pegmatite types is random rather than displaying the regional zonation patterns observed in other belts by Černý (1989). Fuchsloch *et al.* (2018) attributed this random distribution as evidence that the pegmatites are not related to the granites in

https://doi.org/10.1180/mgm.2018.151 Published online by Cambridge University Press

the classical parent–daughter relationship. When comparing the location of the pegmatites studied relative to the granites (Fig. 2) and their individual Ta–Nb- and Sn-oxide fractionation patterns (Fig. 7) there is a similar random distribution of pegmatites with varying degrees of fractionation. This supports the argument that the pegmatites in the Cape Cross–Uis pegmatite belt are not related to the granites in the typical parent–daughter scenario.

Melcher *et al.* (2015) suggested that columbite-group minerals in the Uis pegmatites show concomitant fractionation trends in the columbite quadrilateral based on two of the pegmatites studied in the Cape Cross–Uis pegmatite belt. Contrary to this finding, we suggest that the dominant fractionation trend in the belt is subparallel to the Ta/(Ta + Nb) axis: increasing Ta# with little change in the Mn# (Fig. 8). This trend is typical of beryl-type pegmatites and similar to the Karibib pegmatites studied in Melcher *et al.* (2015). The other pegmatite belts of the Damara Belt are not studied in detail in terms of Ta–Nb oxides, however, Melcher *et al.* (2015), while building an African-scale database, showed that most Ta–Nb oxides are Mn rich and have typical lepidolite-type pegmatite fractionation patterns (e.g. Rubicon, Helicon, Mon Repos and Klein Rössing). The variation in Ta–Nb oxide composition in the Damara Belt may be due to the abundance of F in other pegmatite belts, leading to Mn enrichment (Wise *et al.* 2012). An interesting case is that of the columbite-group minerals fractionation trend in garnet–tourmaline pegmatites, being the only pegmatite type that shows concomitant fractionation, where significant increases in the Mn# occur. Fuchsloch *et al.* (2018) found that garnet–tourmaline pegmatites types have significantly higher abundances of rare-earth elements compared to other pegmatite types within the Cape Cross–Uis pegmatite belt. The authors suggested, that the garnet–tourmaline pegmatites may have a slight NYF pegmatite family affinity and perhaps, although not measured, contain a higher abundance of F compared to other pegmatite types and therefore it may be the cause of Mn-enrichment in columbite-group minerals from these pegmatites. Although Melcher *et al.* (2015) disagree and suggest that there is little difference between the fractionation trends of NYF and LCT pegmatites in Ta–Nb oxides, future detailed studies of coexisting NYF and LCT pegmatites in the same orogenic belt, such as the Damara Belt, might provide some insight into the matter.

Conclusions

Columbite-group minerals and tapiolite fractionation trends, consistent with beryl-to-spodumene rare-element pegmatites, are dominantly controlled by increasing Ta# with little change in the Mn# resulting in a crystallisation sequence of columbite-(Fe) → tantalite-(Fe) → tapiolite. Tapiolite is generally a secondary mineral phase as indicated by its patchy zonation texture. The decrease in minor-element substitution with increasing Ta# in columbite-group minerals and tapiolite, suggests that as new phases began to crystallise in the magma chamber, they competed with columbite-group minerals and tapiolite for these minor elements, and thus their abundances decrease during crystallisation. Unusual bimodal columbite-group minerals fractionation trends and scattered columbite-group mineral data for specific samples were probably due to disequilibrium crystallisation which is supported by textural evidence such as changes in the thickness of oscillatory zones in oscillatory-zoned crystals.

Aqueous fluid vs. highly fractionated magmatic crystallisation of Ta–Nb and Sn oxides has been the subject of appreciable debate. Some authors would argue, based on experimental evidence, that Ta and Nb do not partition into an exsolved pegmatitic aqueous fluid during the late stages of pegmatitic evolution. However, experimental studies are limited and mostly not at pegmatitic conditions (low temperatures of crystallisation) with varying fluid compositions. On the basis of the significantly elevated Ta contents in metasomatised country rocks in contact with pegmatites, compared to low values in unaltered host rocks, we suggest that Ta may have partitioned into an aqueous fluid phase and had a significant effect on Ta–Nb mineralisation together with Sn mineralisation. Ultimately without more experimental evidence, only proxy evidence may be used, and we suggest that future studies on the partition coefficients of Ta into various aqueous fluids at pegmatitic compositions be conducted. Moreover, a more detailed investigation should be carried out on the Cape Cross–Uis host rocks as the current data is limited.

Fractionation levels in columbite-group minerals, tapiolite and cassiterite from specific pegmatites show an irregular spatial distribution relative to granites in the Cape Cross–Uis pegmatite belt. This supports the hypothesis of Fuchsloch *et al.* (2018) that pegmatites were most likely to have been produced from anatexis. If a parent–daughter relationship existed between pegmatites and granites, a distinct zonation pattern surrounding the granitic bodies should be present, with the pegmatites furthest from granites showing the most evolved columbite-group mineral compositions.

Acknowledgements. We thank Deon Van Niekerk for the use and assistance on the Electron Microprobe at Rhodes University (Partially funded by NRF national Equipment Program grant UID 74464). John Spratt was instrumental in this study, confirming early cassiterite results and analysing individual tapiolite crystals at the Natural History Museum, London. We are grateful to the technical team at the University of the Witwatersrand who provided many tireless hours aiding and advising in the separation of accessory minerals. The funding provided by the CIMERA research centre was instrumental to this study, without whom, the project would not have been possible.

Supplementary material. To view supplementary material for this article, please visit https://doi.org/10.1180/mgm.2018.151

References

Alfonso P.A., Corbella M.C. and Melgarejo J.C.D. (1995) Nb-Ta-Minerals from the Cap de Creus pegmatite field, eastern Pyrenees: Distribution and geochemical trends. *Mineralogy and Petrology*, **55**, 53–69.

Alfonso P. and Melgarejo J.C. (2008) Fluid evolution in the zoned rare-element pegmatite field at Cap de Creus, Catalonia, Spain. *The Canadian Mineralogist*, **46**, 597–617.

Ashworth L. (2013) *Mineralised Pegmatites of The Damara Belt, Namibia. Fluid Inclusion and Geochemical Characteristics with Implications of Post Tectonic Mineralisation*. Unpublished PhD thesis, University of the Witwatersrand, Johannesburg.

Ballourad C., Poujol M., Boulvais P., Branquet Y., Tartèse R. and Vigneresse J-L. (2016) Nb-Ta fractionation in peraluminous granites: a marker of the magmatic-hydrothermal transition. *Geology*, **44**, 231–234.

Baumgartner R., Romer R.L. and Moritz R. (2006) Columbite-tantalite-bearing granitic pegmatites from the Seridó belt, northeastern Brazil: genetic constraints from U-Pb dating and Pb isotopes. *The Canadian Mineralogist*, **44**, 69–86.

Beurlen H., Da Silva M.R.R., Thomas R., Soares D.R. and Olivier P. (2008) Nb-Ta-(Ti-Sn) oxide mineral chemistry as tracer of rare-element granitic pegmatite fractionation in the Borborema Province, northeastern Brazil. *Mineralium Deposita*, **43**, 207–228.

Briqueu L., Lancelot J.P., Valois J.P. and Walgenwitz F. (1980) Géochronologie U-Pb d'un type de mineralisation uranifère: les alaskites de Goanikontes (Namibie) 231 et leur encaissant. *Bulletin du Centre de Récherches-Production, Elf-Aquitaine*, **4**, 759–811.

Černý P. (1989) Exploration strategy and methods for pegmatite deposits of tantalum. Pp. 274–310 in: *Lanthanides, Tantalum and Niobium* (P. Möller, P. Černý and F. Saupé, editors) Springer-Verlag, Heidelberg.

Černý P. and Ercit T.S. (1985) Some recent advances in the mineralogy and geochemistry of Nb and Ta in rare-element granitic pegmatites. *Bulletin de Minéralogie*, **108**, 499–532.

Černý P. and Ercit T.S. (1989) Mineralogy of niobium and tantalum: crystal chemical relationships, paragenetic aspects and their economic implications. Pp. 27–79 in: *Lanthanides, Tantalum and Niobium* (P. Moller, P. Černý and F. Saupe, editors) Springer, Berlin, Heidelberg, New York, Tokyo.

Černý P. and Ercit T.S. (2005) The classification of granitic pegmatites revisited. *The Canadian Mineralogist*, **43**, 2005–2026.

Černý P., Chapman R., Chackowsky L.E. and Ercit T.S. (1992*a*) A ferrotantalite-ferrotapiolite intergrowth from Spittal a.d. Drau, Carinthia, Austria. *Mineral Petrology*, **41**, 53–63.

Černý P., Ercit T.S. and Wise M.A. (1992*b*) The tantalite-tapiolite gap: natural assemblages versus experimental data. *The Canadian Mineralogist*, **30**, 587–596.

Černý P., Chapman R., Ferreira K. and Smeds S.-A. (2004) Geochemistry of oxide minerals of Nb, Ta, Sn and Sb in the Varuträsk granitic pegmatite, Swede: The case of an "anomalous" columbite tantalite trend. *American Mineralogist*, **89**, 505–518.

Chevychelov V., Zaraisky C., Borisovskii S. and Borkov D. (2005) Effect of melt composition and temperature on the partitioning of Ta, Nb, Mn and F between granitic (alkaline) melt and fluorine-bearing aqueous fluid: fractionation of Ta and Nb and conditions of ore formation in rare-metal granites. *Petrology*, **13**, 339–357.

De Kock G.S., Eglington B., Armstrong R.A., Harmer R.E. and Walraven F. (2000) U-Pb and Pb-Pb ages of the Naauwpoort rhyolite, Kawakeup leptite and Okongava Diorite: implications for the onset of rifting and orogenesis in the Damara Belt, Namibia. *Communications of the Geological Survey of Namibia, Henno Martin Volume*, **12**, 81–88.

Diehl B.T.M. (1993) Rare metal pegmatites of the Cape Cross – Uis pegmatite belt, Namibia: geology, mineralisation, rubidium-strontium characteristics and petrogenesis. *Journal of African Earth Sciences*, **17**, 167–181.

Ercit T.S., Wise M.A. and Černý P. (1995) Compositional and structural systematics of the columbite group. *American Mineralogist*, **80**, 613–619.

Fuchsloch W.C. (2018) *Pegmatites of the Cape Cross-Uis Pegmatite Belt, Namibia: Structural, Mineralogical, Geochemical and Mineral Chemical Characterisation with Implications for Petrogenesis and Mineralisation.* Unpublished PhD thesis, University of the Witwatersrand, Johannesburg.

Fuchsloch W.C., Nex P.A.M. and Kinnaird J.A. (2018) Classification, mineralogical and geochemical variations in pegmatites of the Cape Cross – Uis pegmatite belt, Namibia. *Lithos*, **296–299**, 79–95.

González T.L., Polonio F.G., Moro F.J.L., Fernández A.F., Contreras J.L.S. and Benito M.C.M. (2017) Tin-tantalum-niobium mineralisation in the Penouta deposit (NW Spain): Textural features and mineral chemistry to unravel the genesis and evolution of cassiterite and columbite group minerals in a peraluminous system. *Ore Geology Reviews*, **81**, 79–95.

Goscombe B., Gray D. and Hand M. (2004) Variation in metamorphic style along the northern margin of the Damara Orogen. *Journal of Petrology*, **45**(6), 1261–1295.

Gray D.R., Foster D.A., Goscombe B., Passchier C.W. and Trouw R.A.J. (2006) $^{40}Ar/^{39}Ar$ thermochronology of the Pan-African Damara Orogen, Namibia, with implications for tectonothermal and geodynamic evolution. *Precambrian Research*, **150**, 49–72.

Haack U. and Gohn E. (1988) Rb-Sr data on some pegmatites in the Damara Orogen, Namibia. *Communications of the Geological Survey of South West Africa/Namibia*, **4**, 13–17.

Hanson S.L., Simmons W.B. and Falster A.U. (1998) Nb-Ta-Ti oxides in granitic pegmatites from the Topsham pegmatite district, Southern Maine. *The Canadian Mineralogist*, **36**, 601–608.

Hoffman P.F., Hawkins D.P., Isachsen C.E. and Bowring S.A. (1996) Precise U-Pb zircon ages for early Damaran magmatism in the Summas Mountains and Welwitschia Inlier, northern Damara Belt, Namibia. *Communications of the Geological Survey of Namibia*, **11**, 47–52.

Keller P., Robles E.R., Pérez A.P. and Fontan F. (1999) Chemistry, paragenesis and significance of tourmaline in pegmatites of the southern Tin Belt, central Namibia. *Chemical Geology*, **158**, 203–225.

Kinnaird J.A. and Nex P.A.M. (2007) A review of geological controls on uranium mineralisation in sheeted leucogranites within the Damara Orogen, Namibia. Trans I.M.M. *Applied Earth Sciences*, **116**(2), 68–85.

Kisters A.F.M. (2005) Controls of gold-quartz vein formation during regional folding in amphibolite-facies, marble-dominated metasediments of the Navachab Gold Mine in the Pan-African Damara Belt, Namibia. *South African Journal of Geology*, **108**, 365–380.

Kovalenko N.I., Ryzhenko B.N., Barsukov V.L., Klintsova A.P., Velyukhanova T.K., Volynets M.P. and Kytayeva L.P. (1986) The solubility of cassiterite in HCl + NaCl(KCl) solutions at 550 °C and 1000 atm under fixed redox conditions. *Geochemistry International*, **23**, 1–16.

Lahti S.I. (1987) Zoning in columbite-tantalite crystals from the granitic pegmatites of the Eräjärvi area, southern Finland. *Geochimica et Cosmochimica Acta*, **51**, 509–517.

Linnen R.L. (1998) The solubility of Nb-Ta-Zr-Hf-W in granitic melts with Li and Li + F: Constraints for mineralisation in rare metal granites and pegmatites. *Economic Geology*, **93**, 1013–1025.

Linnen R.L. and Keppler H. (1997) Columbite solubility in granitic melts: consequences for the enrichment and fractionation of Nb and Ta in the Earth's crust. *Contributions to Mineralogy and Petrology*, **128**, 213–227.

Linnen R.L., Pichavant M. and Holtz F. (1996) The combined effects of fO_2 and melt composition on SnO_2 solubility and tin diffusivity in haplogranitic melts. *Geochimica et Cosmochimica Acta*, **60**, 4965–4976.

London D. (2008) *Pegmatites*. Canadian Mineralogist Special Publication, 10, 347 pp.

Longridge L. (2012) *Tectonothermal Evolution of the Southwestern Central Zone, Damara Belt, Namibia.* Unpublished PhD thesis, University of the Witwatersrand, Johannesburg, 524 pp.

Macey P. and Harris C. (2006) Stable isotope and fluid inclusion evidence for the origin of the Brandberg West area Sn-W vein deposits, NW Namibia. *Mineralium Deposita*, **41**, 671–690.

Martin H. and Porada H. (1977) The intracratonic branch of the Damara Orogen in South West Africa. I. Discussion of geodynamic models. II. Discussion of relationships with the Pan-African Mobile Belt system. *Precambrian Research*, **5**, 311–338 and 339–357.

Martins T., Lima A. and Noronha F. (2009) Evolution trends in columbite-tantalite minerals from pegmatites from the Barroso-Alvão pegmatite field – Northern Portugal. *Estudos Geológicos*, **19**, 212–216.

Melcher F., Graupner T., Gäbler H.-E.Sitnikova M., Henjes-Kunst F., Oberthür T., Gerdes A. and Dewaele S. (2013) Tantalum-(niobium-tin) mineralisation in African pegmatites and rare metal granites: Constraints from Ta-Nb oxide mineralogy, geochemistry and U-Pb geochronology. *Ore Geology Reviews*, **64**, 667–719.

Melcher F., Graupner T., Gäbler H.-E.Sitnikova M., Henjes-Kunst F., Oberthür T., Gerdes A. and Dewaele S. (2015) Tantalum-(niobium-tin) mineralisation in African pegmatites and rare metal granites: Constraints from Ta–Nb oxide mineralogy, geochemistry and U-Pb geochronology. *Ore Geology Reviews*, **64**, 667–719.

Melcher F., Graupner T., Gäbler H.-E.Sitnikova M., Oberthür T., Gerdes A., Badanina E. and Chudy T. (2017) Mineralogical and chemical evolution of tantalum-(niobium-tin) mineralisation in pegmatites and granites. Part 2: Worldwide examples (excluding Africa) and an overview of global metallogenetic patterns. *Ore Geology Reveiws*, **89**, 946–987.

Milani L., Kinnaird J.A., Lehmann J., Naydenov K.V., Saalmann K., Frei D. and Gerdes A. (2015) Role of crustal contribution in the early stage of the Damara Orogen, Namibia: New constraints from combined U-Pb and Lu-Hf isotopes from the Goas Magmatic Complex. *Gondwana Research*, **28**, 961–986.

Miller R.McG. (1983) The Pan-African Damara Orogen of South West Africa/Namibia. Pp. 431–515 in: *The Evolution of the Damara Orogen of South West Africa/Namibia* (R.McG. Miller, editor) Geological Society of South Africa Special Publication, 11.

Miller R.McG. (2008) Neoproterozoic and early Palaeozoic rocks of the Damara Orogen. Pp. 13–1 to 13–410 in: *The Geology of Namibia 2*

https://doi.org/10.1180/mgm.2018.151 Published online by Cambridge University Press

(R.McG. Miller, editor). Ministry of Mines and Energy, Geological Survey, Windhoek.

Miller R.McG. and Frimmel H.E. (2009) Syn- to post-orogenic magmatism. Neoproterozoic evolution of southwestern Africa. Pp. 219–226 in: *Neoproterozoic-Cambrian tectonics, global change and evolution: a focus on southwestern Gondwana* (C. Gaucher, A.N. Sial, G.P. Halverson and H.E. Frimel, editors) Precambrian Geology, **16**.

Mulja T., Williams-Jones A.E., Martin R.F. and Wood S.A. (1996) Compositional variation and structural state of columbite-tantalite in rare-element granitic pegmatites of the Preissac-Lacorne batholith, Quebec, Canada. *American Mineralogist*, **81**, 146–157.

Neiva A.M.R. (1996) Geochemistry of cassiterite and its inclusions and exolutions products from tin and tungsten deposits in Portugal. *The Canadian Mineralogist*, **34**, 745–768.

Novák M. and Černý P. (1998) Niobium-tantalum oxide minerals from complex granitic pegmatites in the Moldanubicum, Czech Republic: primary versus secondary compositional trends. *The Canadian Mineralogist*, **36**, 659–672.

Prave A.R. (1996) Tale of three cratons: tectonostratigraphic anatomy of the Damara Orogen in north-western Namibia and the assembly of Gondwana. *Geology*, **24**, 1115–1118.

Richards T.E. (1986) Geological characteristics of rare-metal pegmatites of the Uis type in the Damara Orogen, South West Africa/Namibia. Pp. 1845–1862 in: *Mineral Deposits of Southern Africa 2* (C.R. Anhaeusser and S. Maske, editors) Society of South Africa, Johannesburg.

Raimbault L. (1998) Compositions of complex lepidolite-type pegmatites and of constituent columbite-tantalite, Chédeville, Massif central, France. *The Canadian Mineralogist*, **36**, 563–583.

Romer R.L. and Lehmann B. (1995) U-Pb columbite age of Neoproterozoic Ta–Nb mineralization in Burundi. *Economic Geology*, **90**, 2303–2309.

Singh P.K. (2007) Tantalite exploration in "Block A" of Uis region, Namibia. *Trabajos de Geologia*, **27**, 41–69.

Singh P.K. (2008) Revelation of tin and niobium occurrences in southern Uis region of Namibia through a geological reconnaissance study. *Trabajos de Geologia*, **28**, 33–39.

Smirnov S.Z., Thomas V.G., Kamenetsky V.S., Kozmenko O.A. and Large R.R. (2012) Hydrosilicate liquids in the system Na_2O-SiO_2-H_2O with NaF, NaCl and Ta: Evaluation of their role in ore and mineral formation at high T and P. *Petrology*, **20**, 271–285.

Smith S.R., Foster L.G., Romer R.L., Tindle A.G., Kelley S.P., Noble S.R., Horstwood M. and Breaks F.W. (2004) U-Pb columbite-tantalite chronology of rare-element pegmatites using TIMS and Laser Ablation-Multi Collector-ICP-MS. *Contributions to Mineralogy and Petrology*, **147**, 549–564.

Splide M.N. and Shearer C.K. (1992) A comparison of tantalum-niobium oxide assemblages in two mineralogically distinct rare-element granitic pegmatites, Black Hills, South Dakota. *The Canadian Mineralogist*, **30**, 719–737.

Swart R. (1992) The sedimentology of the Zerrissene turbidite system, Damara Orogen, Namibia. *Memoirs of the Geological Society of Namibia*, **13**, 54.

Tack L., Williams I. and Bowden P. (2002) SHRIMP constraints on early post collisional granitoids of the Ida Dome, central Damara (Pan-African) Belt, western Namibia. *IAGOD Quadrennial Symposium and Geocongress, Windhoek, Namibia, 11th, abstracts*. Geological Survey of Namibia.

Tindle A.G. and Breaks F.W. (2000) Columbite-tantalite mineral chemistry from rare-element granitic pegmatites: Separation Lake area, N.W. Ontario, Canada. *Mineralogy and Petrology*, **70**, 165–198.

Trompette R. (1997) Neoproterozoic (~600 Ma) aggregation of western Gondwana: a tentative scenario. *Precambrian Research*, **82**, 101–112.

Van Lichtervelde M.V., Beziat S.S.D. and Linnen R.L. (2007) Textural features and chemical evolution in tantalum oxides: magmatic versus hydrothermal origins for Ta mineralization in the Tanco Lower Pegmatite, Manitoba, Canada. *Economic Geology*, **102**, 257–276.

Van Lichtervelde M.V., Grégoire M., Linnen R.L., Béziat D. and Salvi S. (2008) Trace element geochemistry by laser ablation ICPMS of micas associated with Ta mineralization in the Tanco pegmatite, Manitoba, Canada. *Contributions to Mineralogy and Petrology*, **155**, 791–806.

Van Lichtervelde M.V., Grand'Homme A., de Saint-Blanquat M., Olivier P., Gerdes A., Paquette J-L., Melgarejo J.C., Druguet E. and Alfonso P. (2017) U-Pb geochronology on zircon and columbite-group minerals of the Cap de Creus pegmatites, NE Spain. *Mineralogy and Petrology*, **111**, 1–21.

Wagener G.F. (1989) Systematic variation in the tin content of pegmatites in western central Namibia. *Journal of Geochemical Exploration*, **34**, 1–19.

Wise M.A., Francis C.A. and Černý P. (2012) Compositional and structural variations in columbite-group minerals from granitic pegmatites of the Brunswick and Oxford fields, Maine: Differential trends in F-poor and F-rich environments. *The Canadian Mineralogist*, **50**, 1515–1530.

Zhang A.C., Wang R.C., Hu H., Zhang H., Zhu J.C. and Chen X.M. (2004) Chemical evolution of the Nb-Ta oxides and zircon from the Koktokay No. 3 granitic pegmatite, Altai, northwestern China. *Mineralogical Magazine*, **68**, 739–756.

https://doi.org/10.1180/mgm.2018.151 Published online by Cambridge University Press